

Search for high-mass resonances in final states with a τ -lepton and missing transverse momentum with the ATLAS detector

G. Aad *et al.**
(ATLAS Collaboration)

 (Received 27 February 2024; accepted 18 April 2024; published 10 June 2024)

A search for high-mass resonances decaying into a τ -lepton and a neutrino using proton-proton collisions at a center-of-mass energy of $\sqrt{s} = 13$ TeV is presented. The full run 2 data sample corresponding to an integrated luminosity of 139 fb^{-1} recorded by the ATLAS experiment in the years 2015–2018 is analyzed. The τ -lepton is reconstructed in its hadronic decay modes and the total transverse momentum carried out by neutrinos is inferred from the reconstructed missing transverse momentum. The search for new physics is performed on the transverse mass between the τ -lepton and the missing transverse momentum. No excess of events above the Standard Model expectation is observed and upper exclusion limits are set on the $W' \rightarrow \tau\nu$ production cross section. Heavy W' vector bosons with masses up to 5.0 TeV are excluded at 95% confidence level, assuming that they have the same couplings as the Standard Model W boson. For nonuniversal couplings, W' bosons are excluded for masses less than 3.5–5.0 TeV, depending on the model parameters. In addition, model-independent limits on the visible cross section times branching ratio are determined as a function of the lower threshold on the transverse mass of the τ -lepton and missing transverse momentum.

DOI: [10.1103/PhysRevD.109.112008](https://doi.org/10.1103/PhysRevD.109.112008)

I. INTRODUCTION

Multiple theories beyond the Standard Model (SM) predict the existence of additional charged or neutral heavy vector gauge bosons, W' or Z' , that may be observable at the Large Hadron Collider (LHC). The sequential Standard Model (SSM) [1] is a flavor-universal benchmark model that assumes the couplings of the W' and Z' bosons to fermions are identical to those of the W and Z bosons in the SM. Other models that are investigated in this paper are referred to as nonuniversal gauge interaction models (NUGIM) [2–5], which can exhibit different couplings for the three lepton generations.

Searches for new heavy gauge bosons decaying into τ -lepton final states are mainly motivated by models that violate lepton universality, such as the NUGIM. An example is the extension of the electroweak gauge group by an additional SU(2) symmetry group. The first and second generation of fermions can transform under one SU(2) symmetry group, while the third generation of fermions can transform under the additional one. At some energy scale, the extended symmetry is spontaneously

broken to the SM electroweak gauge symmetry and the W' and Z' bosons appear as massive particles. The non-universality of the W' couplings to the SM fermions is parametrized by an angle parameter, θ_{NU} , which is used to scale the couplings to the first and second generations of fermions by $\tan \theta_{\text{NU}}$ and the couplings to the third generation by $\cot \theta_{\text{NU}}$. For $\cot \theta_{\text{NU}} = 1$, the model's couplings are identical to those of the SSM, while values of $\cot \theta_{\text{NU}} > 1$ enhance the couplings to the third generation. The total decay width relative to the W' boson mass in the NUGIM depends on its mass and the value of $\cot \theta_{\text{NU}}$, and it spans from approximately 3% in the SSM limit to 31%–36%, depending on the W' mass, for larger $\cot \theta_{\text{NU}}$.

Alternative models associate the two SU(2) groups with a left-right symmetry [6–8]. The left-symmetry exhibits itself in the electroweak theory and is associated with the parity violation observed in the weak interaction. The right-symmetry has not been observed at the energies probed to date; thus it must be broken at some energy scale and through spontaneous symmetry breaking the new, right-handed W' and Z' bosons become massive.

The ATLAS experiment has searched for W' bosons in the *light-lepton*, $W' \rightarrow \ell\nu$ ($\ell = e, \mu$) [9], and τ -lepton, $W' \rightarrow \tau\nu$ [10], channels. The *light-lepton* searches generally have a better sensitivity than $W' \rightarrow \tau\nu$ for models with universal couplings to fermions because they suffer from less SM background and are enhanced by better lepton reconstruction and identification efficiency. With data collected in the years 2015–2018, corresponding to an

*Full author list given at the end of the article.

Published by the American Physical Society under the terms of the [Creative Commons Attribution 4.0 International license](https://creativecommons.org/licenses/by/4.0/). Further distribution of this work must maintain attribution to the author(s) and the published article's title, journal citation, and DOI. Funded by SCOAP³.

integrated luminosity of 139 fb^{-1} recorded at a center-of-mass energy of $\sqrt{s} = 13 \text{ TeV}$, the ATLAS *light-lepton* search excludes W' bosons in the SSM with masses up to 6.0 TeV [9] at 95% confidence level (CL). The signatures of $W' \rightarrow \tau\nu$ decays in the detectors at LHC are mainly the hadronic decay products of a high-momentum τ -lepton and large missing transverse momentum, due to the prompt neutrino from the W' decay and the neutrino from the subsequent τ -lepton decay. The CMS experiment has searched for $W' \rightarrow \tau\nu$ decays in data collected during the years 2015–2018 and excluded W' bosons in the SSM with masses up to 4.8 TeV [11] at 95% CL. A similar search was performed by the ATLAS experiment in the data collected during the years 2015–2016, amounting to 36.1 fb^{-1} of integrated luminosity, and excluded W' bosons in the SSM with masses up to 3.7 TeV [10] at 95% CL.

Exclusion limits on the masses of the new heavy gauge bosons as a function of the parameter $\cot\theta_{\text{NU}}$ can also be derived by indirect searches. The most stringent limits are derived from electroweak precision measurements (EWPT) [12] and by the absence of lepton flavor violation (LFV) in the SM [13]. They exclude W' bosons with masses below 1.8 – 2.5 TeV , depending on the coupling. Weaker limits can be set either from tests of the unitarity of the Cabibbo–Kobayashi–Maskawa (CKM) matrix [14] or Z-pole data [2].

In this paper, a search for $W' \rightarrow \tau\nu$ decays with the full run 2 ATLAS data sample, corresponding to an integrated luminosity of 139 fb^{-1} , recorded with the ATLAS detector in proton–proton collisions at a center-of-mass energy of $\sqrt{s} = 13 \text{ TeV}$ at the LHC is presented. In this analysis, events were selected using missing transverse momentum triggers and the τ -leptons are exclusively reconstructed in their hadronic decay modes, which account for 65% of all τ -lepton decays. Compared to the previous ATLAS search, this analysis is making use of the additional data collected between the years 2017–2018, the improvements in the reconstruction and identification of the τ -leptons at ATLAS, as well as the strategy of a multibin search approach.

II. ATLAS DETECTOR

The ATLAS detector [15–17] at the LHC is a multipurpose particle detector with a forward-backward symmetric cylindrical geometry and a near 4π coverage in solid angle.¹ It consists of an inner tracking detector surrounded by a thin superconducting solenoid providing a 2 T axial magnetic field, electromagnetic (EM) and hadron calorimeters,

¹ATLAS uses a right-handed coordinate system with its origin at the nominal interaction point (IP) in the center of the detector and the z -axis along the beam pipe. The x -axis points from the IP to the center of the LHC ring, and the y -axis points upwards. Cylindrical coordinates (r, ϕ) are used in the transverse plane, ϕ being the azimuthal angle around the z -axis. The pseudorapidity is defined in terms of the polar angle θ as $\eta = -\ln \tan(\theta/2)$. Angular distance is measured in units of $\Delta R \equiv \sqrt{(\Delta\eta)^2 + (\Delta\phi)^2}$.

and a muon spectrometer. The inner tracking detector covers the pseudorapidity range $|\eta| < 2.5$. It consists of silicon pixel, silicon microstrip, and transition radiation tracking detectors. Lead/liquid-argon (LAr) sampling calorimeters provide EM energy measurements with high granularity. A steel/scintillator-tile hadron calorimeter covers the central pseudorapidity range ($|\eta| < 1.7$). The end cap and forward regions are instrumented with LAr calorimeters for both the EM and hadronic energy measurements up to $|\eta| = 4.9$. The muon spectrometer surrounds the calorimeters and is based on three large superconducting air-core toroidal magnets with eight coils each. The field integral of the toroids ranges between 2.0 and 6.0 Tm across most of the detector. The muon spectrometer includes a system of precision tracking chambers and fast detectors for triggering. A two-level trigger system is used to select events [18,19]. The first-level trigger is implemented in hardware and uses a subset of the detector information to accept events at a rate below 100 kHz. This is followed by a software-based high-level trigger (HLT) that reduces the accepted event rate to 1 kHz on average depending on the data-taking conditions.

An extensive software suite [20] is used in data simulation, in the reconstruction and analysis of real and simulated data, in detector operations, and in the trigger and data acquisition systems of the experiment.

III. SIGNAL AND BACKGROUND SAMPLES

Signal events of $W' \rightarrow \tau\nu$ decays were generated at leading order with the PYTHIA 8.212 [21] event generator and the NNPDF2.3LO parton distribution function (PDF) set [22]. The A14 set of tuned parameters (*tune*) [23] was used to simulate the parton shower and the hadronization process. The TAUOLA v2.9 package [24] was used for the simulation of the τ -lepton decays.

The W' signal events were generated with invariant mass of the $\tau\nu$ system above 25 GeV . The event generation used an artificially biased phase space sampling to generate more events at high invariant masses. Signal events for various resonance masses in the range of 500 GeV to 6000 GeV were modeled by reweighting this sample using a leading-order matrix-element (ME) calculation. For the NUGIM signals, depending on the values of $\cot\theta_{\text{NU}}$ and resonance mass, the total decay width of the W' bosons increased up to 36%, which affects the signal acceptance. W' decays into boson pairs (WZ , Wh) were neglected in the calculation of the total decay width. This impacts the total decay width by less than 7%. Very large values of $\cot\theta_{\text{NU}}$ (>5.5) are not studied as the model becomes nonperturbative in this region. The signal cross section is corrected to account for next-to-next-to-leading-order (NNLO) quantum chromodynamics (QCD) effects by mass-dependent k -factors. The NNLO QCD effects in the k -factors were calculated using VRAP v0.9 [25] and the CT14NNLO PDF set [26]. Electroweak corrections as well as interference

TABLE I. Details of the generators and software packages used to simulate the background samples, including the generation of the matrix element and the corresponding PDF set as well as the modeling of nonperturbative effects such as parton showers, PDF set and MC tune.

Process	Generator	ME order	PDF	Parton shower	Tune
$W/Z + \text{jets}$	POWHEG BOX v1 [33–36]	NLO	CT10NLO [37]	PYTHIA 8.186 + CTEQ 6L1 [38]	AZNLO [39]
$t\bar{t}$	POWHEG BOX v2 [33–35,40]	NLO	NNPDF3.0NLO [41]	PYTHIA 8.230 + NNPDF2.3LO	A14
Single top	POWHEG BOX v2 [33–35,42]	NLO	NNPDF3.0NLO	PYTHIA 8.230 + NNPDF2.3LO	A14
Diboson	SHERPA 2.2.1 or 2.2.2 [43]	MEPS@NLO [44]	NNPDF3.0NNLO [41]	SHERPA [44–49]	SHERPA
$Z(\rightarrow \nu\nu) + \text{jets}$	SHERPA 2.2.1	MEPS@NLO	NNPDF3.0NNLO	SHERPA	SHERPA

between W and W' bosons are expected to be model-dependent and are not considered.

The SM background to this search is divided into events where the selected τ -lepton candidate originates from a quark- or gluon-initiated jet (*jet background*) and those where it does not (*nonjet background*). The jet background is primarily due to $W/Z + \text{jets}$, mainly $Z(\rightarrow \nu\nu) + \text{jets}$, and multijet production and is estimated from data. The nonjet background is estimated by using simulation and mainly originates from $W \rightarrow \tau\nu$ production. Additionally, smaller contributions come from $W/Z/\gamma^*$ decays into leptonic final states, top-quark ($t\bar{t}$ and single top-quark) production, and diboson (WW , WZ , and ZZ) production, collectively referred to as *other background*. The generators and software packages used for the simulation of the background samples are summarized in Table I. In addition, quantum electrodynamics (QED) final-state radiation in $W/Z/\gamma^*$ processes was simulated with PHOTOS++ 3.52 [27,28]. Decays of bottom and charm hadrons were simulated with EVTGEN 1.2.0 and EVTGEN 1.6.0 [29] for $W/Z/\gamma^*$ and top quark processes, respectively. For diboson and $Z(\rightarrow \nu\nu) + \text{jets}$ production, virtual QCD corrections to matrix elements at next-to-leading-order (NLO) accuracy were provided by the OPENLOOPS library [30–32].

All simulated Monte Carlo (MC) events were processed through a simulation of the detector geometry and response [50] using the GEANT4 framework [51]. The effect of multiple interactions in the same and neighboring bunch crossings (pileup) was modeled by overlaying the simulated hard-scattering event with inelastic proton-proton (pp) events generated with PYTHIA 8.186 [52] and the A3 tune [53]. The average number of pileup interactions (additional pp collisions in the same or adjacent bunch crossings) observed in the analyzed data is about 33. All MC samples are reweighted so that the distribution of the number of collisions per bunch crossing matches that observed in data. They are normalized using the integrated luminosity of the data sample and the cross sections calculated at NNLO in QCD and NLO for electroweak processes. The NNLO QCD and NLO electroweak effects are included in the simulated $W/Z/\gamma^*$ samples by applying mass-dependent k -factors. The electroweak correction effects are calculated using MCSANC [54] in the case of QED effects due to initial-state radiation,

interference between initial- and final-state radiation, and Sudakov logarithm single-loop corrections. The software used for the reconstruction is the same for both simulated and real data.

IV. ANALYSIS STRATEGY AND EVENT SELECTION

The efficient selection of high-mass $W' \rightarrow \tau\nu$ decays and the suppression of backgrounds requires an accurate identification of hadronic τ -lepton decays, the reconstruction of their transverse momentum and the reconstruction of the missing transverse momentum, which are used to build the final discriminating variable for this search.

The interaction vertices from pp collisions are reconstructed from inner detector tracks with transverse momenta $p_{\text{T}}^{\text{track}} > 0.5$ GeV that originate from the beam collision region in the transverse plane. In presence of several primary vertices, the hard-scatter primary vertex is chosen as the interaction vertex with the highest sum of squared $p_{\text{T}}^{\text{track}}$. Events with no hard-scatter primary vertex are rejected. Additionally, the candidate events are required to satisfy standard data-quality criteria [55].

The τ -lepton is reconstructed from its hadronic decay products. Hadronic τ -lepton decays are composed of a neutrino and a set of visible decay products ($\tau_{\text{had-vis}}$), typically one or three charged pions and up to two neutral pions. The reconstruction of the visible decay products is seeded by jets reconstructed from topological clusters [56] of energy depositions in the calorimeter. The reconstruction of $\tau_{\text{had-vis}}$ candidates is detailed in Refs. [57,58].

The $\tau_{\text{had-vis}}$ candidates are required to have transverse momentum, $p_{\text{T}}^{\tau_{\text{had-vis}}} > 30$ GeV and $|\eta| < 2.4$ (excluding the region $1.37 < |\eta| < 1.52$). They are required to have one (1-prong) or three (3-prong) associated tracks within the *core region* of $\Delta R < 0.2$ around the $\tau_{\text{had-vis}}$ axis and an electric charge of $|Q| = 1$. The prompt charged-particle tracks within the *core region* are classified using boosted decision trees (BDT) against other tracks that can originate from other sources (such as tracks from photon conversions, underlying events or pileup), which increases the reconstruction efficiency of the high- p_{T} $\tau_{\text{had-vis}}$ relative to the previous analysis.

Only the candidate with the highest transverse momentum in the event is selected.

Hadronic τ -lepton decays are identified with a recurrent neural network (RNN) algorithm [59] based on calorimetric shower shape and tracking information to suppress backgrounds from quark- or gluon-initiated jets that are reconstructed as τ -lepton candidates. Since the jet background for high W' masses is small, loose criteria are used for the τ -lepton identification to maintain a high signal efficiency. The chosen *loose* working point of the τ -lepton identification has an efficiency of 85% for 1-prong candidates and 75% for 3-prong candidates. At the same time, the *loose* working point provides a jet background rejection factor of at least 21 for 1-prong candidates and 90 for 3-prong candidates. For the separation of 1-prong τ -lepton candidates from misidentified electrons, a dedicated discriminant based on a BDT [58] is used with an efficiency of 95% and an electron background rejection factor of 50–100, depending on the pseudorapidity.

Events with a reconstructed electron [60] or muon [61] are rejected. This lepton veto makes use of *loose* electron and muon identification criteria and considers lepton candidates with transverse momenta above 20 GeV. The electrons are required to be reconstructed with $|\eta| < 2.47$ (excluding $1.37 < |\eta| < 1.52$) while muons are required to be reconstructed with $|\eta| < 2.5$. Electrons and muons are required to have tracks associated with the primary vertex with longitudinal impact parameter $|z_0 \sin \theta| < 0.5$ mm and transverse impact parameter significance $|d_0/\sigma(d_0)| < 5$ for electrons and $|d_0/\sigma(d_0)| < 3$ for muons, where $\sigma(d_0)$ is the measured uncertainty in d_0 .

Jet candidates are reconstructed from topological clusters of energy deposition in the calorimeter [56] using the anti- k_r algorithm [62,63] with a radius parameter $R = 0.4$. They are calibrated using simulation with corrections obtained from *in situ* techniques in data [64]. Jets are required to have a transverse momentum above 20 GeV and a pseudorapidity in the range of $|\eta| < 4.5$. To reduce the effect of pileup on jets with transverse momenta less than 60 GeV, the jet vertex tagging (JVT) and forward jet vertex tagging (fJVT) algorithms [65,66] are used for jets with $|\eta| < 2.5$ and $2.5 < |\eta| < 4.5$, respectively, to determine the likelihood of the jet originating from the hard-scattering vertex. Jets enter indirectly in the analysis through the calculation of the missing transverse momentum of the event.

The events are required to satisfy criteria designed to reduce noncollision backgrounds from cosmic rays, single-beam-induced events and calorimeter noise [67]. To further suppress single-beam-induced background, the $\tau_{\text{had-vis}}$ candidate must have at least one associated track with transverse momentum greater than 10 GeV.

The missing transverse momentum with magnitude $E_{\text{T}}^{\text{miss}}$ is calculated as the negative vectorial sum of the transverse momenta of all reconstructed objects in the event. In addition, a *soft term* [68] is added to account for

the contribution from tracks that originate from the primary vertex but are not associated with the reconstructed objects.

Events were selected by triggers that required $E_{\text{T}}^{\text{miss}}$ to be above a threshold of 70, 90 or 110 GeV, depending on the data-taking period [69]. The offline-reconstructed $E_{\text{T}}^{\text{miss}}$ is required to be at least 150 GeV, motivated by the high W' masses (~ 0.5 –6 TeV) considered in this search, to suppress multijet background and to minimize the uncertainty in the trigger efficiency. The trigger efficiency for this offline threshold is about 80% and increases to more than 99% for $E_{\text{T}}^{\text{miss}} > 200$ GeV. Single τ -lepton triggers were not used because they provide similar offline thresholds as the $E_{\text{T}}^{\text{miss}}$ triggers, but also include a τ -lepton identification step at the HLT. The latter can result in a bias in the data selection and consequently the jet background estimation, which is described in Sec. V.

Correction factors are applied to simulation to account for differences observed in the detector response between data and MC. This includes corrections for the τ -lepton reconstruction and identification efficiencies, as well as the energy and momentum scales and resolutions of the reconstructed objects [58,64,70]. Additional corrections are derived for τ -lepton candidates with $p_{\text{T}}^{\tau_{\text{had-vis}}}$ above 100 GeV that have a long flight length in the detector since the direct interaction of τ -leptons with the detector is not included in the simulation. More than 50% of the τ -leptons with $p_{\text{T}}^{\tau_{\text{had-vis}}} > 100$ GeV decay after a flight distance of 30 mm in the transverse plane, which corresponds to the innermost layer of the ATLAS detector. The corrections are determined by comparing the reconstruction and identification efficiencies for the selected $W' \rightarrow \tau\nu$ sample with a dedicated simulated sample that includes direct interactions of τ -leptons with the detector. The missing transverse momentum trigger efficiencies are measured with $Z(\rightarrow \mu\mu) + \text{jets}$ events, where the jet is reconstructed as a τ -lepton candidate, exploiting the fact that muons typically deposit only a small fraction of their energy in the calorimeter. The trigger efficiencies are measured in data and simulation after removing the muons from the $E_{\text{T}}^{\text{miss}}$ calculation, which results in similar event topologies to those studied in this paper.

Additional kinematic selection criteria are applied to further reduce multijet background. As the W' bosons are typically produced with low transverse momenta, the τ -lepton and the neutrino from the W' decay are produced back-to-back in the transverse plane and have approximately balanced transverse momenta. Due to the large W' mass and the resulting boost of the τ -lepton and its decay products, the direction of the neutrino from the τ -lepton decay is close to the original direction of the τ -lepton. The neutrino from the τ -lepton decay thus partially cancels the missing transverse momentum caused by the prompt neutrino from the W' decay. As a result, the $\tau_{\text{had-vis}}$ candidate and the missing transverse momentum are also preferentially balanced. Therefore, the azimuthal angle between the τ -lepton candidate and the missing transverse

TABLE II. Summary of the event selection requirements. The top part of the table summarizes the “preselection” requirements that apply to all regions used in this analysis. The bottom part shows the additional selection requirements for each individual region. Here, the symbol L stands for *loose* τ -lepton identification and VL\L denotes the requirement that the τ -lepton candidate must satisfy the *very loose* but fail to satisfy the *loose* identification.

Preselection					
E_T^{miss} trigger	70, 90, 110 GeV				
Event cleaning	Applied				
$\tau_{\text{had-vis}}$ tracks	1 or 3				
$\tau_{\text{had-vis}}$ charge	± 1				
$p_T^{\tau_{\text{had-vis}}}$	> 30 GeV				
$\tau_{\text{had-vis}}$ $p_T^{\text{leadTrack}}$	> 10 GeV				
Lepton veto	applied				
$\Delta\phi_{\tau_{\text{had-vis}}, E_T^{\text{miss}}}$	> 2.4 rad				
Region requirements					
	SR	CR1	CR2	CR3	VR
τ -lepton identification	L	VL\L	L	VL\L	L
E_T^{miss}	> 150 GeV	> 150 GeV	< 100 GeV	< 100 GeV	> 150 GeV
$p_T^{\tau_{\text{had-vis}}} / E_T^{\text{miss}}$	$\in [0.7, 1.3]$	$\in [0.7, 1.3]$	< 0.7
m_T	> 240 GeV

momentum, $\Delta\phi_{\tau_{\text{had-vis}}, E_T^{\text{miss}}}$, is required to be larger than 2.4 radians and their transverse momentum ratio to be in the range of $0.7 < p_T^{\tau_{\text{had-vis}}} / E_T^{\text{miss}} < 1.3$.

The selection criteria discussed above define the *signal region* (SR) of the $W' \rightarrow \tau\nu$ search. The selection acceptance times efficiency, $\mathcal{A} \times \varepsilon$, is approximately 8% for a low-mass resonance with $m_{W'_{\text{SSM}}} = 500$ GeV and is mainly affected by the trigger and E_T^{miss} requirements of the SR. For higher resonance masses near 2.5 TeV, the $\mathcal{A} \times \varepsilon$ increases to approximately 25%. Due to the event selection requirements and the increased production of off shell W' bosons at lower invariant mass, the selection $\mathcal{A} \times \varepsilon$ decreases for $m_{W'_{\text{SSM}}}$ above 3 TeV and reaches approximately 16% for resonance masses at 6 TeV. An overview of the selected event yields is given in Table III. A summary of the event selection and the region requirements is given in Table II. In addition to the SR, three *control regions* (CR1, CR2 and CR3), as defined in Sec. V, are used to obtain a data-driven estimate of the jet background and a

validation region (VR) is used to validate the SM background in the high- m_T region.

The transverse mass of the reconstructed $\tau_{\text{had-vis}}$ candidate and E_T^{miss} , m_T , defined as

$$m_T = \sqrt{2E_T^{\text{miss}} p_T^{\tau_{\text{had-vis}}} (1 - \cos \Delta\phi_{\tau_{\text{had-vis}}, E_T^{\text{miss}}})} \quad (1)$$

is used to further separate the signal from backgrounds as a high-mass W' is expected to produce events at higher m_T values. Due to the presence of the additional neutrino from the τ -lepton decay, the distribution of the transverse mass for the signal process is not expected to show a Jacobian peak. The separation between signal and background uses a profile likelihood based on the m_T distribution, as described in Sec. VII.

V. JET BACKGROUND ESTIMATION

While all nonjet backgrounds in this analysis are estimated by using simulation, the jet background is estimated

TABLE III. Overview of the selected numbers of events for data, the SM backgrounds and a W'_{SSM} signal of mass 5 TeV. The jet background is estimated from data and cannot be quantified before the requirements of $E_T^{\text{miss}} > 150$ GeV and τ -lepton identification. “Preselection” denotes all selection criteria described in Sec. IV except for the τ -lepton identification, E_T^{miss} and $p_T^{\tau_{\text{had-vis}}} / E_T^{\text{miss}}$ requirements. The last row summarizes the number of observed and expected events above a large m_T threshold but is not part of the SR selection. The quoted uncertainties include both statistical and systematic sources of uncertainty.

Selection	Data	$W \rightarrow \tau\nu$	Jet background	Other background	W'_{SSM} (5 TeV)
Preselection	3 640 749	$102\,000 \pm 6\,000$...	$73\,000 \pm 6\,000$	18 ± 5
τ -lepton identification	1 189 863	$84\,000 \pm 5\,000$...	$52\,000 \pm 4\,000$	17 ± 4
$E_T^{\text{miss}} > 150$ GeV	58 528	$13\,400 \pm 1\,600$	$31\,000 \pm 9\,000$	$12\,000 \pm 1\,500$	15 ± 4
$0.7 < \frac{p_T^{\tau_{\text{had-vis}}}}{E_T^{\text{miss}}} < 1.3$	18 528	$9\,700 \pm 1\,400$	$5\,800 \pm 400$	$2\,900 \pm 500$	14 ± 4
$m_T > 1$ TeV	58	51 ± 12	10 ± 4	12.0 ± 2.7	7.2 ± 3.3

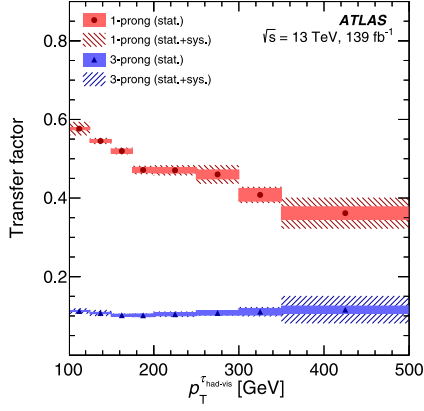


FIG. 1. Transfer factors used in the jet-background estimation as a function of $p_T^{\tau_{\text{had-vis}}}$, for 1-prong (circles) and 3-prong (upward triangles) τ -lepton decays. The uncertainty due to the limited number of events in CR2 and CR3 is shown as solid filled areas while the hatched areas indicates the total statistical and systematic uncertainties.

by using a data-driven approach since the misidentification of jets as τ -lepton candidates is not well modeled by the simulation. In this approach, the jet background is determined from data events that fail to satisfy the τ -lepton identification requirement of the signal region and is transferred to the signal region using dedicated *transfer factors* measured in independent control regions.

Three control regions are defined. The events in the first control region (CR1) are required to satisfy the same selection criteria as for the signal region but fail to satisfy *loose* and satisfy *very loose* τ -lepton identification. The *very loose* τ -lepton identification working point corresponds to a 95% signal efficiency and 9.9 and 16 background rejection factors for 1-prong and 3-prong $\tau_{\text{had-vis}}$ candidates, respectively. The other two control regions are enriched in dijet events. For the definition of these regions, the requirement on

$p_T^{\tau_{\text{had-vis}}} / E_T^{\text{miss}}$ is removed, and the missing transverse momentum must not exceed 100 GeV, while the other selection criteria remain the same as for the signal region. For one of these two control regions the τ -lepton candidate must satisfy *loose* τ -lepton identification (CR2), while for the other it must fail to satisfy *loose* but satisfy *very loose* τ -lepton identification (CR3). In all three control regions, the nonjet background is subtracted using simulation. The signal contamination in all three regions is small and is neglected.

The transfer factors, F_{ij} , correspond to the ratio of events in CR2 and CR3 and are shown in Fig. 1. They are measured in intervals of $p_T^{\tau_{\text{had-vis}}}$ (denoted by index i), and separately for 1-prong and 3-prong τ -lepton candidates (denoted by index j). Further dependence on other observables, such as the $\tau_{\text{had-vis}}$ η or the event's trigger, is found to give negligible effects and is not considered. The transfer factors measured in the $p_T^{\tau_{\text{had-vis}}}$ interval of 350 to 500 GeV are also used for reweighting events with $p_T^{\tau_{\text{had-vis}}}$ above 500 GeV. The number of jet background events in the signal region, $N_{\text{SR}}^{\text{jet}}$, is computed from the number of data events in CR1 using these transfer factors,

$$N_{\text{SR}}^{\text{jet}} = \sum_{i,j} (N_{\text{CR1},ij}^{\text{data}} - N_{\text{CR1},ij}^{\text{nonjet}}) F_{ij},$$

$$\text{where } F_{ij} = \frac{N_{\text{CR2},ij}^{\text{data}} - N_{\text{CR2},ij}^{\text{nonjet}}}{N_{\text{CR3},ij}^{\text{data}} - N_{\text{CR3},ij}^{\text{nonjet}}}, \quad (2)$$

and $N_{X,ij}^{\text{data}}$ ($N_{X,ij}^{\text{nonjet}}$) corresponds to the number of data (simulated) events populating the i th and j th intervals of $p_T^{\tau_{\text{had-vis}}}$ and number of prongs, respectively, in the region $X \in \{\text{CR1}, \text{CR2}, \text{CR3}\}$. The jet background estimate is validated in a VR with $p_T^{\tau_{\text{had-vis}}} / E_T^{\text{miss}} < 0.7$ and $m_T > 240$ GeV. The data and estimated backgrounds are found to be compatible within the uncertainties, as shown in Fig. 2.

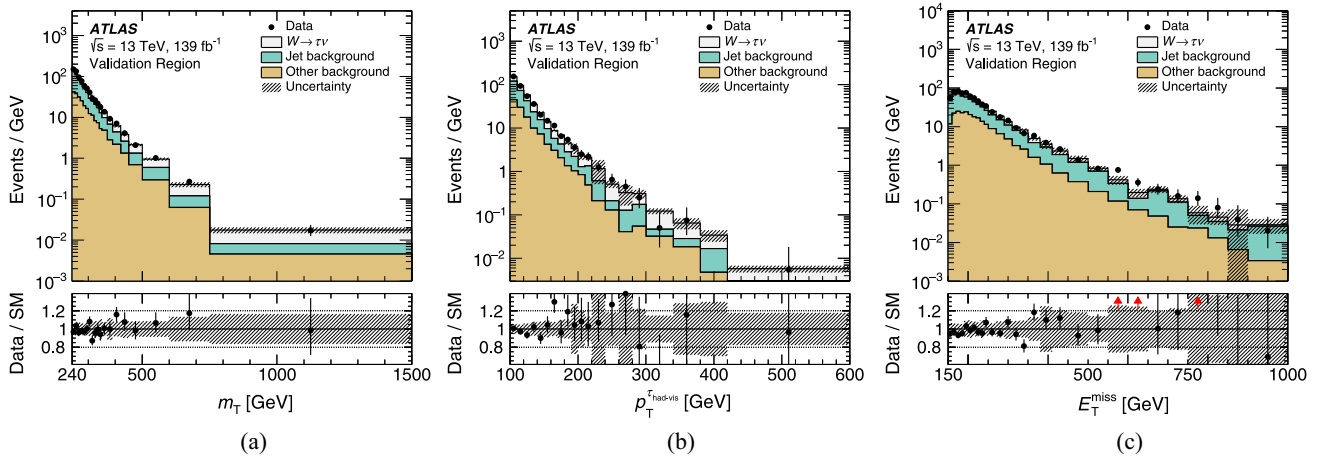


FIG. 2. Distributions of (a) the transverse mass, m_T , (b) the transverse momentum of the $\tau_{\text{had-vis}}$ candidate, $p_T^{\tau_{\text{had-vis}}}$, and (c) the missing transverse momentum in the event, E_T^{miss} , in the validation region. The uncertainty band (hatched) shows the total statistical and systematic uncertainty. Arrows in lower panels indicate data points that lie outside the vertical range of the axis.

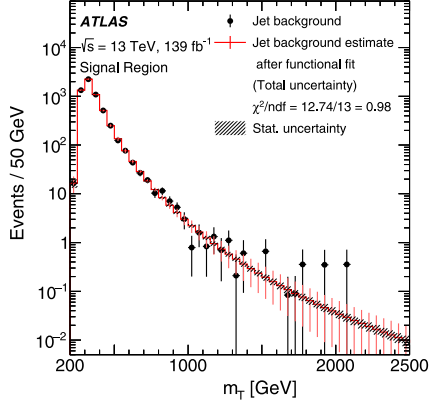


FIG. 3. Distribution of the transverse mass, m_T , of the jet background estimate. The markers represent the jet background as estimated from applying the transfer factor to the data in CR1. The line shows the binned jet background obtained from the functional fit in the range 500–1200 GeV and its extrapolation for m_T values above 1200 GeV. The hashed area represents the statistical uncertainty and the vertical lines show the total uncertainty of the jet background estimate.

Due to the small number of events at high m_T in CR1, where the signal events are located, a function of the form $f(m_T) = Am_T^B$ with free parameters A and B is fitted to the m_T distribution in the range of $450 < m_T < 1200$ GeV. This function is used to parametrize the background shape for $m_T > 500$ GeV and is extrapolated for $m_T > 1200$ GeV. Effects arising from kinematic suppressions, such as from the parton distribution functions, are neglected in this simple extrapolation, as the jet background for $m_T > 1200$ GeV contributes to less than 15% of the total SM background and does not affect the analysis results. Figure 3 shows the m_T distribution of the jet background

estimate before and after performing the functional fit. The statistical uncertainty in the fitted function is determined by pseudo-experiments from the jet background distribution and performing a fit with the same function.

The data and estimated backgrounds are found to be compatible within the uncertainties for all observables used for the event selection. Figure 4 shows the distributions of the $\tau_{\text{had-vis}}$ transverse momentum, the missing transverse momentum in the event, and the azimuthal angle between the $\tau_{\text{had-vis}}$ candidate and the missing transverse momentum, in the signal region.

The estimation of the jet background is based on the assumption that the derived transfer factors calculated from control regions are applicable for the signal region. Systematic uncertainties are assigned to account for any residual correlations between the transfer factor and the E_T^{miss} criteria in the control region definitions that would arise if the jet composition differs between CR1 and CR2/CR3. They are evaluated by repeating the jet background estimation using modified control region definitions. The lower E_T^{miss} thresholds are varied from 0 to 70 GeV and the upper threshold from 100 to 150 GeV, and the largest difference in each bin is taken as systematic uncertainty. The statistical uncertainty in the transfer factor measurement is propagated from the control regions into the signal regions by using pseudoexperiments. The uncertainty from the subtraction of nonjet contamination in the control regions is found to be small and corresponds to an uncertainty in the jet background yields in the m_T distribution of 2%–5%. The uncertainty due to differences between the quark/gluon fraction of CR1 and CR3 is found to impact the jet background yields in the m_T distribution by 3%–13%. It is determined by reweighting the data in CR1 before obtaining the jet background estimate.

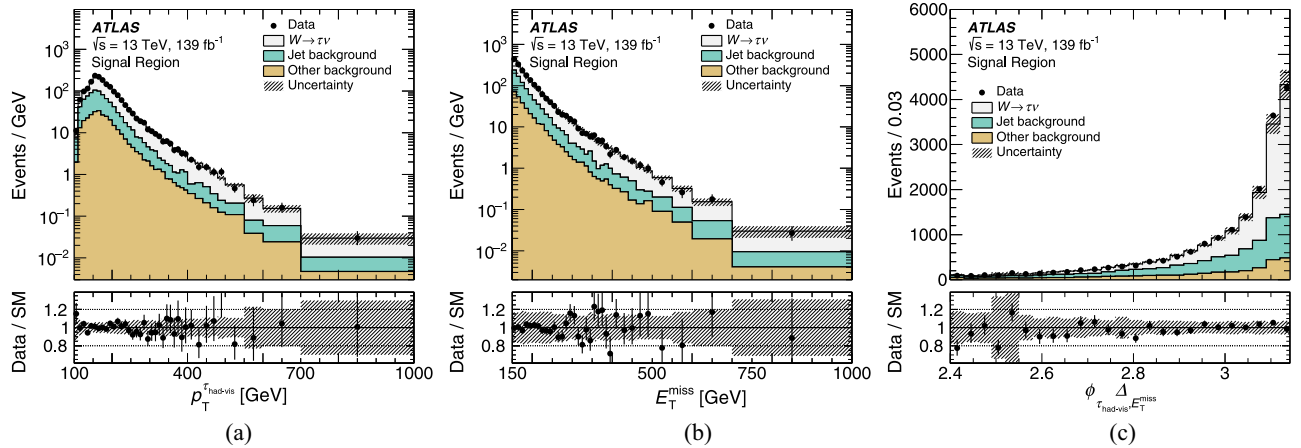


FIG. 4. Distributions of (a) the transverse momentum of the $\tau_{\text{had-vis}}$ candidate, $p_T^{\tau_{\text{had-vis}}}$, (b) the missing transverse momentum in the event, E_T^{miss} , and (c) the azimuthal angle between the $\tau_{\text{had-vis}}$ candidate and the missing transverse momentum, $\Delta\phi_{\tau_{\text{had-vis}}, E_T^{\text{miss}}}$, in the signal region. The uncertainty band (hatched) shows the total statistical and systematic uncertainty.

TABLE IV. Summary of the uncertainties in the jet background estimate. The “...” symbol indicates that the uncertainty source is not applicable in the relevant m_T range.

Systematic uncertainty	Relative uncertainty in the jet background [%]	
	200 GeV < m_T < 300 GeV	$m_T > 2000$ GeV
Nonjet background subtraction	+2/−3	+2/−17
Variation of E_T^{miss} thresholds	±2	±16
Quark/gluon ratio differences	±3	±13
Extrapolation of transfer factor	±2	±16
Alternative fit function	...	±58
Lower fit range ±50 GeV	...	±19
Higher fit range ±50 GeV	...	±2
m_T rebinning	...	±2

The reweighting is performed such that the distribution of the τ -lepton candidate’s jet seed width² has a similar shape for the two regions. The reweighting is also parametrized as a function of the τ -lepton candidate’s $p_T^{\text{had-vis}}$ and the number of associated tracks used to capture the transfer factor differences.

The uncertainty from applying a constant transfer factor for $p_T^{\text{had-vis}} > 350$ GeV is determined from a recalculation of the transfer factors for an extension of the measurement to transverse momenta of 1 TeV. The uncertainty due to the extrapolation of the jet background estimate for $m_T > 500$ GeV is evaluated by comparing the nominal estimate with the one obtained when modifying the functional form using an alternative fit function ($f(m_T) = Am_T^{B+C \log m_T}$, with free parameters A , B , and C), which also yields a good fit quality. Additional extrapolation uncertainties are considered by varying the lower and upper boundaries of the fit range of the functional form by ±50 GeV and rebinning the m_T distribution of the jet background before performing the functional fit. The total uncertainty in the jet background estimate ranges from 4% at $m_T = 200$ GeV to 94% at $m_T = 2$ TeV, where, however, the jet background level is low. For low m_T the uncertainty is mainly due to the subtraction of nonjet background contamination, while for high m_T , above 800 GeV, is mainly due to the alternative fit function.

A summary of the systematic uncertainties in the jet background estimate for different m_T regions is given in Table IV.

VI. SYSTEMATIC UNCERTAINTIES

The uncertainties in the data-driven estimate of the jet background have already been discussed in Sec. V. In this section, the systematic uncertainties due to reconstruction effects and the uncertainties of simulated nonjet background modeling are discussed. Specifically, uncertainties in the detector simulation impact the reconstruction,

²The τ -lepton candidate’s jet seed width corresponds to the width of the jet that seeded the τ -lepton reconstruction.

identification and trigger efficiencies as well as the energy scales and resolutions of reconstructed objects.

The uncertainty in the $\tau_{\text{had-vis}}$ energy scale is 3%–4% [58]. The impact of this uncertainty is found to vary with m_T , from 2% at $m_T = 200$ GeV to 10% at $m_T = 2$ TeV for a signal with $m_{W_{\text{SSM}}} = 5$ TeV, from 10% to 40% for $W \rightarrow \tau\nu$ and from 15% to 45% for the other backgrounds. It is the overall largest systematic uncertainty for the simulated backgrounds. The uncertainty in the τ -lepton identification efficiency is 5%–6%, as determined from measurements of $Z \rightarrow \tau\tau$ events. For higher transverse momenta outside of the range that can be probed with $Z \rightarrow \tau\tau$ decays, an additional uncertainty that increases by 9% per TeV for 1-prong and 6% per TeV for 3-prong candidates is used, in accordance with studies of high transverse-momentum jets [71]. The uncertainty in the electron veto efficiency is found to be 2%, independent of m_T .

The uncertainty in the factors used to correct for the absence of direct interactions of τ -leptons with the detector material in the simulation is due to the limited number of the generated events and to small differences between the nominal correction factors and those obtained from an alternative simulated sample ($\gamma^* \rightarrow \tau\tau$). This impacts the m_T distribution of the simulated signal and SM backgrounds, with uncertainty that varies from 0.5% at $m_T = 200$ GeV to 2% at $m_T = 3$ TeV. The E_T^{miss} trigger efficiency has an uncertainty of about 5% for offline-reconstructed E_T^{miss} of 150 GeV that decreases to below 1% for larger E_T^{miss} values. It is determined by the statistical uncertainties in the trigger correction factors measured in the $Z(\rightarrow \mu\mu) + \text{jets}$ events and from the difference between correction factors measured in $W(\rightarrow \mu\nu) + \text{jets}$ and $t\bar{t}$ events. The overall impact of the trigger scale factor uncertainties (statistical and systematic) on the signal and background yields is 10% at low m_T and becomes negligible above 1 TeV.

Although jets are not directly used in this analysis, their energy scale and resolution uncertainties affect the E_T^{miss} reconstruction and lead to variations of the background yields of 1%–2% for signal and $W \rightarrow \tau\nu$ and 2%–10% for

the other simulated backgrounds. In addition, uncertainties related to the scale and resolution of the missing transverse energy soft term are evaluated. They lead to variations of 0.5%–2% for signal and backgrounds, depending on m_T . Uncertainties associated with the reconstruction of electrons and muons have a negligible impact.

The uncertainty of the combined integrated luminosity for the period 2015–2018 is 1.7% [72], obtained using the LUCID-2 detector [73] for the primary luminosity measurements. The impact of the uncertainties on the pileup contribution in simulation yields a systematic uncertainty of less than 1% for signal and simulated backgrounds.

Theoretical uncertainties in the W and Z/γ^* differential production cross sections arise from PDF uncertainties, the uncertainty in the value of the strong coupling constant, α_s , and higher-order corrections. The strong coupling constant is varied to 0.118 [74] from the nominal value of $\alpha_s(m_Z) = 0.13$ used in the CT14NNLO PDF set. Additional uncertainties are estimated by simultaneously varying up and down the renormalization (μ_R) and factorization (μ_F) scales of the CT14NNLO PDF set by a factor of 2. A single nuisance parameter is used to quantify the uncertainty due to the PDF. It is evaluated by the 90% CL eigenvector variations of the CT14NNLO PDF as described in Ref. [75]. An additional uncertainty is derived due to the choice of the nominal PDF set, by comparing the values of CT14NNLO to those of ATLAS-epWZ16 [76] and NNPDF3.0 PDFs, following standard prescriptions as in Ref. [75]. The maximum absolute deviation from the envelope of these comparisons is used as the PDF choice uncertainty, when it is larger than the CT14NNLO PDF eigenvector variation envelope. The uncertainty in the electroweak correction is assessed by comparing the multiplicative scheme $[(1 + \delta_{\text{QCD}}) \times (1 + \delta_{\text{EW}})]$ with the additive scheme $(\delta_{\text{QCD}} + \delta_{\text{EW}})$, where the NNLO QCD corrections, δ_{QCD} , and the NLO electroweak corrections, δ_{EW} , are determined as described in Ref. [9]. The additive approach is taken as the nominal value and its difference from the multiplicative approach is taken as a symmetric uncertainty. For the Z/γ^* processes, an uncertainty to the photon-induced correction is derived by the taking into account uncertainties of the photon PDF and quark masses. The total cross section uncertainty, once the theory uncertainties are combined in quadrature, varies with the transverse mass from 5% (at $m_T = 200$ GeV) to 20% (at $m_T = 3$ TeV) for $W \rightarrow \tau\nu$ and from 2% to 20% for the other backgrounds, as they contain $W \rightarrow \ell\nu$ and neutral-current Drell–Yan processes. For the $W' \rightarrow \tau\nu$ signal, the theory uncertainty increases from 4% to 50% with m_T and W' mass. The theory uncertainty is not applied on the signal.

The $t\bar{t}$ cross section has been calculated to NNLO and has an uncertainty of 5%–6% [77,78]. The single-top cross sections (s , t and Wt channels) have uncertainties of 3%–5% [79,80]. Uncertainties due to the modeling of hard scattering, fragmentation, interference and additional

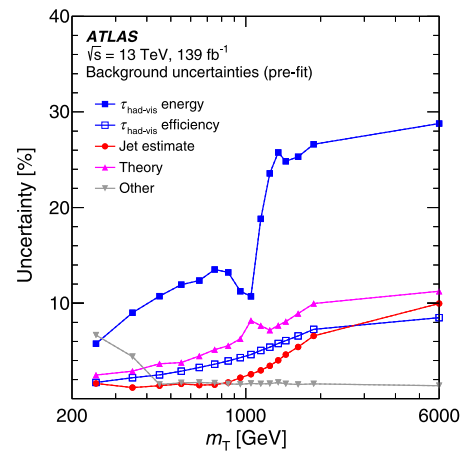


FIG. 5. Relative systematic uncertainties (in %) on the total background yield before the likelihood fit to data (*pre-fit*) as a function of m_T . The filled squares show the uncertainty due to the τ -lepton energy scale, the open squares show the uncertainties originating from the τ -lepton reconstruction and identification efficiencies, the circles show the uncertainty originating from the jet background estimation, and the upward triangles show the uncertainty from the simulated background cross sections. Additional sources of uncertainty, such as those from the trigger efficiency measurement, the jet energy scale and the luminosity, are combined in the downward arrows.

radiation for the top-quark processes are also considered. They are determined by comparing alternative MC samples with different settings. A cross section uncertainty of 10% is used for diboson production [81,82] and of 5% for $Z(\rightarrow \nu\nu) + \text{jets}$ production [83]. All these result in a total uncertainty in the other background of approximately 10%–15%.

The impact of these systematic uncertainties in the total background yields as a function of m_T is shown in Fig. 5.

VII. RESULTS

For the statistical analysis of the data, a profile-likelihood fit to the m_T distributions of signal and background is performed. For the signal, binned m_T distributions for a series of W' masses in the range of $500 \text{ GeV} < m_{W'} < 6000 \text{ GeV}$ are used. A profile-likelihood ratio is used as the test statistic. The likelihood functions in the ratio are products of Poisson probabilities over all bins in the m_T distribution. Systematic uncertainties are included in the fit as nuisance parameters constrained by Gaussian prior probability density functions. The theory uncertainties in the signal are not included as nuisance parameters but are shown as an uncertainty band on the predicted W' cross section. In the numerator of the likelihood ratio, the likelihood function is maximized assuming the presence of a signal above the expected background, while in the denominator the background-only hypothesis is assumed. Upper 95% CL limits on the signal normalization are derived using a modified frequentist confidence level

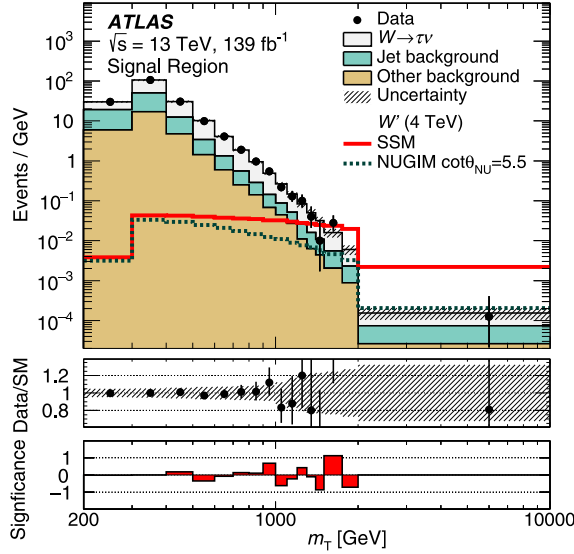


FIG. 6. Distribution of the transverse mass, m_T , in the signal region after the likelihood fit to data (*postfit*) under the background-only hypothesis. The uncertainty band (hatched) shows the total statistical and systematic uncertainty. The m_T distributions of a W' signal with mass of 4 TeV within the SSM (red solid line) and NUGIM with $\cot\theta_{\text{NU}} = 5.5$ (dark green dotted line) are overlaid. The significance of the data given the SM expectation and its uncertainty is given in the lower panel. It is determined independently per bin and is computed as described in Ref. [86].

$\text{CL}_s = \frac{p_{s+b}}{1-p_b}$ [84]. The p -values for the signal-plus-background (p_{s+b}) and background-only (p_b) hypotheses are determined using asymptotic formulas [85].

The m_T distribution after the profile-likelihood fit to data under the background-only hypothesis is shown in Fig. 6. There is good agreement between the data and total background estimates. Since no significant deviation from the SM expectation is observed, upper limits on the cross sections for the different signal mass hypotheses are derived. The exclusion limits on the product of cross section and branching fraction for $W' \rightarrow \tau\nu$ as a function of the W' mass in the SSM are shown in Fig. 7(a). This search excludes the signal for W' masses up to 5.0 TeV at 95% CL. The expected limit is 4.9 TeV. For high signal masses (>4 TeV), the validity of the asymptotic formulas was tested against pseudoexperiments, resulting in an increase of the observed upper limits of less than 8%. The analysis for W' boson masses above 2 TeV remains statistically limited and would benefit from increased integrated luminosity and improved reconstruction of high- p_T $\tau_{\text{had-vis}}$.

Upper exclusion limits on the production cross section times branching ratio are also determined for NUGIM with $1 \leq \cot\theta_{\text{NU}} \leq 5.5$. W' bosons with masses in the range of 3.5 to 5.0 TeV, depending on $\cot\theta_{\text{NU}}$, are excluded at 95% CL as shown in Fig. 7(b).

The calculation of the upper limits for the SSM and NUGIM assume certain shapes of the m_T distributions for

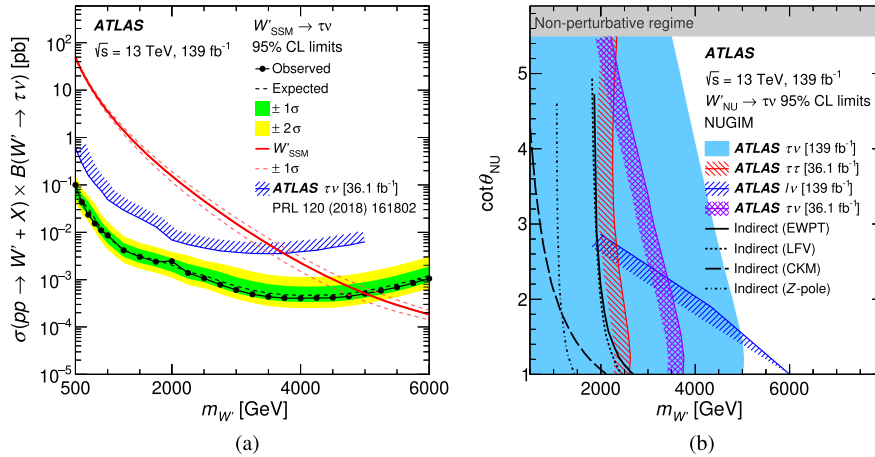


FIG. 7. (a) Observed (black markers) and expected (black dashed line) 95% CL upper limits on the cross section times branching ratio ($\sigma \times \mathcal{B}$) as a function of the W' mass in the SSM. The inner and outer bands show the ± 1 and ± 2 standard deviations, respectively, of the expected limit. The solid red line represents the theoretical cross section and the dashed red lines represent its theoretical uncertainty for the SSM signal. The blue hatched line indicates the observed 95% CL upper limits on $\sigma \times \mathcal{B}$ of the previous ATLAS $\tau\nu$ [10] search. (b) Observed 95% CL lower limit on the W' mass as a function of the parameter $\cot\theta_{\text{NU}}$ describing the coupling to the third generation. The blue shaded area represents the exclusion limits set by this analysis of the full run 2 data sample of ATLAS. For the same data sample, the exclusion limits set by the $W' \rightarrow \ell\nu$ search [9] are also shown as blue forward hatched line. The observed limits from the previous ATLAS $\tau\nu$ [10] (purple diagonal crosses) and $\tau\tau$ [71] (red backward hatched line) searches with 36.1 fb^{-1} are overlaid for comparison. The W' and Z' bosons are assumed to be degenerate in mass. Indirect limits at 95% CL from fits to electroweak precision measurements (EWPT) [12], lepton flavor violation (LFV) [13], CKM unitarity [14] and the Z-pole data [2] are also overlaid.

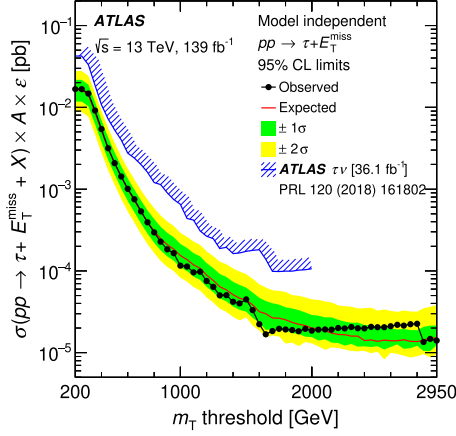


FIG. 8. Model-independent 95% CL upper limits on the visible $\tau + E_T^{\text{miss}}$ cross section as a function of the transverse mass thresholds, m_T^{thresh} . The blue hatched line shows the observed 95% CL upper limits on the visible $\tau + E_T^{\text{miss}}$ cross section of the previous ATLAS $\tau\nu$ [10] search. The steps in the observed upper limit at m_T^{thresh} of 1.6 and 2.85 TeV result of the discrete nature of the data and that the highest m_T event in data appeared with $m_T = 2.83$ TeV.

the signal. However, alternative models that also result in a τ -lepton + E_T^{miss} final state can have different signal shapes. For this reason, model-independent limits are provided, which are calculated as upper limits on the signal yields above certain transverse mass thresholds, m_T^{thresh} , from 0.2 TeV to 2.95 TeV. For m_T^{thresh} above 1.5 TeV the limits are calculated using pseudo-experiments because the expected and observed numbers of events drop considerably. Figure 8 shows the 95% CL upper limits on the visible cross section, $\sigma(pp \rightarrow \tau + E_T^{\text{miss}} + X) \times \mathcal{A} \times \epsilon$, as a function of m_T^{thresh} . Good agreement between the generated and reconstructed m_T distributions is observed; hence the m_T^{thresh} acceptance can be determined at generator level. General models resulting in larger visible cross sections for τ -lepton + E_T^{miss} production than the determined upper limits are excluded by this analysis. Thus, this analysis excludes possible signals with visible cross sections larger than 17 fb for $m_T^{\text{thresh}} = 0.2$ TeV and 0.014 fb for $m_T^{\text{thresh}} = 2.95$ TeV. Compared to previous results, this improves the upper limits on the visible cross section for $m_T^{\text{thresh}} > 1.5$ TeV by a factor of 5.

The improvements in the limits compared to the previous analysis are mainly due to the increased size of the data sample, an improved τ -lepton identification as well as the BDT-based track association to τ -lepton candidates and the multibin search approach.

VIII. CONCLUSION

A search for $W' \rightarrow \tau\nu$ decays in 139 fb^{-1} of pp collisions at a center-of-mass energy of $\sqrt{s} = 13$ TeV recorded with the ATLAS detector at the Large Hadron

Collider is presented. The analysis is performed with hadronic τ -lepton decays. The signal is searched for in the transverse mass spectrum and no excess above the Standard Model expectation is observed. Exclusion limits are set on the cross section for W' production in the sequential Standard Model as a function of the W' mass. W' masses up to 5.0 TeV are excluded at 95% confidence level. This result improves upon the limits obtained in the previous $W' \rightarrow \tau\nu$ analysis from ATLAS, based on a data sample of 36.1 fb^{-1} , by 1.3 TeV. W' bosons in models with nonuniversal couplings are excluded for masses less than 3.5–5.0 TeV, depending on the model parameters. Additionally, model-independent upper limits on the visible production cross section for $\tau + E_T^{\text{miss}}$ are derived and range from 17 fb for a lower transverse mass threshold of $m_T^{\text{thresh}} = 200$ GeV to 0.014 fb for $m_T^{\text{thresh}} = 2.95$ TeV.

ACKNOWLEDGMENTS

We thank CERN for the very successful operation of the LHC and its injectors, as well as the support staff at CERN and at our institutions worldwide without whom ATLAS could not be operated efficiently. The crucial computing support from all WLCG partners is acknowledged gratefully, in particular from CERN, the ATLAS Tier-1 facilities at TRIUMF/SFU (Canada), NDGF (Denmark, Norway, Sweden), CC-IN2P3 (France), KIT/GridKA (Germany), INFN-CNAF (Italy), NL-T1 (Netherlands), PIC (Spain), RAL (UK) and BNL (USA), the Tier-2 facilities worldwide and large non-WLCG resource providers. Major contributors of computing resources are listed in Ref. [87]. We gratefully acknowledge the support of ANPCyT, Argentina; YerPhI, Armenia; ARC, Australia; BMWFW and FWF, Austria; ANAS, Azerbaijan; CNPq and FAPESP, Brazil; NSERC, NRC and CFI, Canada; CERN; ANID, Chile; CAS, MOST and NSFC, China; Minciencias, Colombia; DNRF and DNSRC, Denmark; IN2P3-CNRS and CEA-DRF/IRFU, France; SRNSFG, Georgia; BMBF, HGF and MPG, Germany; RGC and Hong Kong SAR, China; ISF and Benozio Center, Israel; INFN, Italy; MEXT and JSPS, Japan; CNRST, Morocco; NWO, Netherlands; RCN, Norway; MEiN, Poland; FCT, Portugal; MNE/IFA, Romania; MESTD, Serbia; MSSR, Slovakia; ARRS and MIZŠ, Slovenia; DSI/NRF, South Africa; MICINN, Spain; SRC and Wallenberg Foundation, Sweden; SERI, SNSF and Cantons of Bern and Geneva, Switzerland; MOST, Taipei; STFC, United Kingdom; DOE and NSF, United States of America. Individual groups and members have received support from BCKDF, CANARIE, CRC and DRAC, Canada; PRIMUS 21/SCI/017 and UNCE SCI/013, Czech Republic; COST, ERC, ERDF, Horizon 2020 and Marie Skłodowska-Curie Actions, European Union; Investissements d'Avenir Labex, Investissements d'Avenir IDEX and ANR, France; DFG and AvH Foundation, Germany; Herakleitos, Thales and Aristeia programmes cofinanced by EU-ESF and the Greek NSRF, Greece;

BSF-NSF and MINERVA, Israel; Norwegian Financial Mechanism 2014-2021, Norway; La Caixa Banking Foundation, CERCA Programme Generalitat de Catalunya and PROMETEO and GenT Programmes Generalitat Valenciana, Spain; Göran Gustafssons Stiftelse, Sweden; The Royal Society and Leverhulme Trust, United Kingdom. In addition, individual members wish to acknowledge support from CERN: CERN & Society Foundation (ATLAS PhD Grant); Chile: Agencia Nacional de Investigación y Desarrollo (Grants No. FONDECYT 1190886, No. FONDECYT 1210400); China: National Natural Science Foundation of China (Grant No. NSFC-12075060), EU: H2020 European Research Council (Grant No. H2020-MSCA-IF-2020: HPOFHC—10103); European Union: European Research Council (Grant No. ERC—948254), Horizon 2020 Framework Programme (MUCCA—CHIST-ERA-19-XAI-00); France: Agence Nationale de la Recherche (Grant No. ANR-21-CE31-0022); Germany: Deutsche Forschungsgemeinschaft (Grant No. DFG—CR 312/5-1); Italy: Istituto Nazionale di Fisica Nucleare (FELLINI G.A. Grant No.. 754496); Poland:

Polish National Agency for Academic Exchange (Grant No. PPN/PPO/2020/1/00002/U/00001), Polish National Science Centre (Grants No. NCN UMO-2019/34/E/ST2/00393, No. UMO-2020/37/B/ST2/01043); South Africa: South Africa National Research Foundation (Grant No. CPRR118515); Spain: Generalitat Valenciana (Grants No. APOSTD/2019/165, No. PGC2018-094856-BI00, Artemisa, FEDER, IDIFEDER/2018/048), La Caixa Banking Foundation (La Caixa Foundation, Grants No. LCF/BQ/PI19/11690014, No. LCF/BQ/PI20/11760025), PROMETEO and GenT Programmes Generalitat Valenciana (Grants No. CIDEAGENT/2019/023, No. CIDEAGENT/2019/027, No. CIDEAGENT/2019/029, No. GVA-SEJI/2020/037); Sweden: Swedish Research Council (Grant No. SRC—2017-05160, VR 2017-05092), Knut and Alice Wallenberg Foundation (Grants No. KAW 2017.0100, No. KAW 2018.0157, No. KAW 2019.0447); Switzerland: Swiss National Science Foundation (Grant No. SNSF—PCEFP2_194658); United Kingdom: Leverhulme Trust (Leverhulme Trust Grant No. RPG-2020-004).

-
- [1] G. Altarelli, B. Mele, and M. Ruiz-Altaba, Searching for new heavy vector bosons in $p\bar{p}$ colliders, *Z. Phys. C* **45**, 109 (1989).
- [2] E. Malkawi, T. Tait, and C.-P. Yuan, A model of strong flavor dynamics for the top quark, *Phys. Lett. B* **385**, 304 (1996).
- [3] D. J. Muller and S. Nandi, Top flavor: A separate $SU(2)$ for the third family, *Phys. Lett. B* **383**, 345 (1996).
- [4] K. Hsieh, K. Schmitz, J.-H. Yu, and C.-P. Yuan, Global analysis of general $SU(2) \times SU(2) \times U(1)$ models with precision data, *Phys. Rev. D* **82**, 035011 (2010).
- [5] C.-W. Chiang, N. G. Deshpande, X.-G. He, and J. Jiang, Family $SU(2)_l \times SU(2)_h \times U(1)$ model, *Phys. Rev. D* **81**, 015006 (2010).
- [6] C.-F. Chang and E. Ma, Flavor changing neutral currents in the asymmetric left-right gauge model, *J. High Energy Phys.* **09** (2018) 058.
- [7] K. S. Babu, B. Dutta, and R. N. Mohapatra, A theory of $R(D^*, D)$ anomaly with right-handed currents, *J. High Energy Phys.* **01** (2019) 168.
- [8] A. Greljo, D. J. Robinson, B. Shakya, and J. Zupan, $R(D^{(*)})$ from W' and right-handed neutrinos, *J. High Energy Phys.* **09** (2018) 169.
- [9] ATLAS Collaboration, Search for a heavy charged boson in events with a charged lepton and missing transverse momentum from pp collisions at $\sqrt{s} = 13$ TeV with the ATLAS detector, *Phys. Rev. D* **100**, 052013 (2019).
- [10] ATLAS Collaboration, Search for high-mass resonances decaying to $\tau\nu$ in pp collisions at $\sqrt{s} = 13$ TeV with the ATLAS detector, *Phys. Rev. Lett.* **120**, 161802 (2018).
- [11] CMS Collaboration, Search for new physics in the τ lepton plus missing transverse momentum final state in proton-proton collisions at $\sqrt{s} = 13$ TeV, *J. High Energy Phys.* **09** (2023) 051.
- [12] Q.-H. Cao, Z. Li, J.-H. Yu, and C.-P. Yuan, Discovery and identification of W' and Z' in $SU(2)_1 \otimes SU(2)_2 \otimes U(1)_X$ models at the LHC, *Phys. Rev. D* **86**, 095010 (2012).
- [13] K. Y. Lee, Lepton flavor violation in a nonuniversal gauge interaction model, *Phys. Rev. D* **82**, 097701 (2010).
- [14] K. Y. Lee, Unitarity violation of the CKM matrix in a nonuniversal gauge interaction model, *Phys. Rev. D* **71**, 115008 (2005).
- [15] ATLAS Collaboration, The ATLAS experiment at the CERN Large Hadron Collider, *J. Instrum.* **3**, S08003 (2008).
- [16] ATLAS Collaboration, ATLAS insertable B-layer: Technical design report, Reports No. ATLAS-TDR-19, No. CERN-LHCC-2010-013, 2010, <https://cds.cern.ch/record/1291633>, Addendum: ATLAS-TDR-19-ADD-1; Report No. CERN-LHCC-2012-009, 2012, <https://cds.cern.ch/record/1451888>.
- [17] B. Abbott *et al.*, Production and integration of the ATLAS insertable B-layer, *J. Instrum.* **13**, T05008 (2018).
- [18] ATLAS Collaboration, Performance of the ATLAS trigger system in 2015, *Eur. Phys. J. C* **77**, 317 (2017).
- [19] ATLAS Collaboration, Operation of the ATLAS trigger system in Run 2, *J. Instrum.* **15**, P10004 (2020).
- [20] ATLAS Collaboration, The ATLAS Collaboration software and firmware, Report No. ATL-SOFT-PUB-2021-001, 2021, <https://cds.cern.ch/record/2767187>.

- [21] T. Sjöstrand, R. Corke, N. Desai, P. Ilten, S. Mrenna, S. Prestel, Christine O. Rasmussen, and Peter Z. Skands, An introduction to PYTHIA 8.2, *Comput. Phys. Commun.* **191**, 159 (2015).
- [22] NNPDF Collaboration, Parton distributions with LHC data, *Nucl. Phys.* **B867**, 244 (2013).
- [23] ATLAS Collaboration, ATLAS Pythia 8 tunes to 7 TeV data, Report No. ATL-PHYS-PUB-2014-021, 2014, <https://cds.cern.ch/record/1966419>.
- [24] S. Jadach, J. H. Kühn, and Z. Was, TAUOLA—a library of Monte Carlo programs to simulate decays of polarized τ leptons, *Comput. Phys. Commun.* **64**, 275 (1991).
- [25] C. Anastasiou, L. Dixon, K. Melnikov, and F. Petriello, High-precision QCD at hadron colliders: Electroweak gauge boson rapidity distributions at next-to-next-to leading order, *Phys. Rev. D* **69**, 094008 (2004).
- [26] S. Dulat, T.-J. Hou, J. Gao, M. Guzzi, J. Huston, P. Nadolsky, J. Pumplin, C. Schmidt, D. Stump, and C.-P. Yuan, New parton distribution functions from a global analysis of quantum chromodynamics, *Phys. Rev. D* **93**, 033006 (2016).
- [27] P. Golonka and Z. Was, PHOTOS Monte Carlo: A precision tool for QED corrections in Z and W decays, *Eur. Phys. J. C* **45**, 97 (2006).
- [28] N. Davidson, T. Przedzinski, and Z. Was, PHOTOS interface in C++: Technical and physics documentation, *Comput. Phys. Commun.* **199**, 86 (2016).
- [29] D. J. Lange, The EvtGen particle decay simulation package, *Nucl. Instrum. Methods Phys. Res., Sect. A* **462**, 152 (2001).
- [30] F. Buccioni, J.-N. Lang, J. M. Lindert, P. Maierhöfer, Stefano Pozzorini, Hantian Zhang, and Max F. Zoller, OpenLoops 2, *Eur. Phys. J. C* **79**, 866 (2019).
- [31] F. Cascioli, P. Maierhöfer, and S. Pozzorini, Scattering amplitudes with open loops, *Phys. Rev. Lett.* **108**, 111601 (2012).
- [32] A. Denner, S. Dittmaier, and L. Hofer, Collier: A fortran-based complex one-loop library in extended regularizations, *Comput. Phys. Commun.* **212**, 220 (2017).
- [33] P. Nason, A new method for combining NLO QCD with shower Monte Carlo algorithms, *J. High Energy Phys.* **11** (2004) 040.
- [34] S. Frixione, P. Nason, and C. Oleari, Matching NLO QCD computations with parton shower simulations: The POWHEG method, *J. High Energy Phys.* **11** (2007) 070.
- [35] S. Alioli, P. Nason, C. Oleari, and E. Re, A general framework for implementing NLO calculations in shower Monte Carlo programs: The POWHEG BOX, *J. High Energy Phys.* **06** (2010) 043.
- [36] S. Alioli, P. Nason, C. Oleari, and E. Re, NLO vector-boson production matched with shower in POWHEG, *J. High Energy Phys.* **07** (2008) 060.
- [37] H.-L. Lai, M. Guzzi, J. Huston, Z. Li, P. M. Nadolsky, J. Pumplin, and C.-P. Yuan, New parton distributions for collider physics, *Phys. Rev. D* **82**, 074024 (2010).
- [38] J. Pumplin, D. R. Stump, J. Huston, H.-L. Lai, P. Nadolsky, and W.-K. Tung, New generation of parton distributions with uncertainties from global QCD analysis, *J. High Energy Phys.* **07** (2002) 012.
- [39] ATLAS Collaboration, Measurement of the Z/γ^* boson transverse momentum distribution in pp collisions at $\sqrt{s} = 7$ TeV with the ATLAS detector, *J. High Energy Phys.* **09** (2014) 145.
- [40] S. Frixione, G. Ridolfi, and P. Nason, A positive-weight next-to-leading-order Monte Carlo for heavy flavour hadroproduction, *J. High Energy Phys.* **09** (2007) 126.
- [41] NNPDF Collaboration, Parton distributions for the LHC run II, *J. High Energy Phys.* **04** (2015) 040.
- [42] E. Re, Single-top Wt -channel production matched with parton showers using the POWHEG method, *Eur. Phys. J. C* **71**, 1547 (2011).
- [43] E. Bothmann *et al.*, Event generation with Sherpa 2.2, *SciPost Phys.* **7**, 034 (2019).
- [44] S. Höche, F. Krauss, M. Schönherr, and F. Siegert, QCD matrix elements + parton showers. The NLO case, *J. High Energy Phys.* **04** (2013) 027.
- [45] T. Gleisberg and S. Höche, Comix, a new matrix element generator, *J. High Energy Phys.* **12** (2008) 039.
- [46] S. Schumann and F. Krauss, A parton shower algorithm based on Catani–Seymour dipole factorisation, *J. High Energy Phys.* **03** (2008) 038.
- [47] S. Höche, F. Krauss, M. Schönherr, and F. Siegert, A critical appraisal of NLO + PS matching methods, *J. High Energy Phys.* **09** (2012) 049.
- [48] S. Catani, F. Krauss, B. R. Webber, and R. Kuhn, QCD matrix elements + parton showers, *J. High Energy Phys.* **11** (2001) 063.
- [49] S. Höche, F. Krauss, S. Schumann, and F. Siegert, QCD matrix elements and truncated showers, *J. High Energy Phys.* **05** (2009) 053.
- [50] ATLAS Collaboration, The ATLAS simulation infrastructure, *Eur. Phys. J. C* **70**, 823 (2010).
- [51] S. Agostinelli *et al.*, GEANT4—a simulation toolkit, *Nucl. Instrum. Methods Phys. Res., Sect. A* **506**, 250 (2003).
- [52] T. Sjöstrand, S. Mrenna, and P. Skands, A brief introduction to PYTHIA 8.1, *Comput. Phys. Commun.* **178**, 852 (2008).
- [53] ATLAS Collaboration, The Pythia 8 A3 tune description of ATLAS minimum bias and inelastic measurements incorporating the Donnachie–Landshoff diffractive model, Report No. ATL-PHYS-PUB-2016-017, 2016, <https://cds.cern.ch/record/2206965>.
- [54] A. Arbuzov, D. Bardin, S. Bondarenko, P. Christova, L. Kalinovskaya, U. Klein, V. Kolesnikov, L. Romyantsev, R. Sadykov, and A. Sapronov, Update of the MCSANC Monte Carlo integrator, v. 1.20, *JETP Lett.* **103**, 131 (2016).
- [55] ATLAS Collaboration, ATLAS data quality operations and performance for 2015–2018 data-taking, *J. Instrum.* **15**, P04003 (2020).
- [56] ATLAS Collaboration, Topological cell clustering in the ATLAS calorimeters and its performance in LHC Run 1, *Eur. Phys. J. C* **77**, 490 (2017).
- [57] ATLAS Collaboration, Identification and energy calibration of hadronically decaying tau leptons with the ATLAS experiment in pp collisions at $\sqrt{s} = 8$ TeV, *Eur. Phys. J. C* **75**, 303 (2015).
- [58] ATLAS Collaboration, Measurement of the tau lepton reconstruction and identification performance in the ATLAS experiment using pp collisions at $\sqrt{s} = 13$ TeV, Report

- No. ATLAS-CONF-2017-029, 2017, <https://cds.cern.ch/record/2261772>.
- [59] ATLAS Collaboration, Identification of hadronic tau lepton decays using neural networks in the ATLAS experiment, Report No. ATL-PHYS-PUB-2019-033, 2019, <https://cds.cern.ch/record/2688062>.
- [60] ATLAS Collaboration, Electron and photon performance measurements with the ATLAS detector using the 2015–2017 LHC proton–proton collision data, *J. Instrum.* **14**, P12006 (2019).
- [61] ATLAS Collaboration, Muon reconstruction and identification efficiency in ATLAS using the full Run 2 pp collision data set at $\sqrt{s} = 13$ TeV, *Eur. Phys. J. C* **81**, 578 (2021).
- [62] M. Cacciari, G. P. Salam, and G. Soyez, The anti- k_r jet clustering algorithm, *J. High Energy Phys.* **04** (2008) 063.
- [63] M. Cacciari, G. P. Salam, and G. Soyez, FastJet user manual, *Eur. Phys. J. C* **72**, 1896 (2012).
- [64] ATLAS Collaboration, Jet energy scale and resolution measured in proton–proton collisions at $\sqrt{s} = 13$ TeV with the ATLAS detector, *Eur. Phys. J. C* **81**, 689 (2021).
- [65] ATLAS Collaboration, Performance of pile-up mitigation techniques for jets in pp collisions at $\sqrt{s} = 8$ TeV using the ATLAS detector, *Eur. Phys. J. C* **76**, 581 (2016).
- [66] ATLAS Collaboration, Identification and rejection of pile-up jets at high pseudorapidity with the ATLAS detector, *Eur. Phys. J. C* **77**, 580 (2017); **77**, 712(E) (2017).
- [67] ATLAS Collaboration, Selection of jets produced in 13 TeV proton–proton collisions with the ATLAS detector, Report No. ATLAS-CONF-2015-029, 2015, <https://cds.cern.ch/record/2037702>.
- [68] ATLAS Collaboration, E_T^{miss} performance in the ATLAS detector using 2015–2016 LHC pp collisions, Report No. ATLAS-CONF-2018-023, 2018, <https://cds.cern.ch/record/2625233>.
- [69] ATLAS Collaboration, Performance of the missing transverse momentum triggers for the ATLAS detector during Run-2 data taking, *J. High Energy Phys.* **08** (2020) 080.
- [70] ATLAS Collaboration, Performance of missing transverse momentum reconstruction with the ATLAS detector using proton–proton collisions at $\sqrt{s} = 13$ TeV, *Eur. Phys. J. C* **78**, 903 (2018).
- [71] ATLAS Collaboration, Search for additional heavy neutral Higgs and gauge bosons in the ditau final state produced in 36 fb^{-1} of pp collisions at $\sqrt{s} = 13$ TeV with the ATLAS detector, *J. High Energy Phys.* **01** (2018) 055.
- [72] ATLAS Collaboration, Luminosity determination in pp collisions at $\sqrt{s} = 13$ TeV using the ATLAS detector at the LHC, Report No. ATLAS-CONF-2019-021, 2019, <https://cds.cern.ch/record/2677054>.
- [73] G. Avoni *et al.*, The new LUCID-2 detector for luminosity measurement and monitoring in ATLAS, *J. Instrum.* **13**, P07017 (2018).
- [74] S. Dulat, T.-J. Hou, J. Gao, M. Guzzi, J. Huston, P. Nadolsky, J. Pumplin, C. Schmidt, D. Stump, and C.-P. Yuan, New parton distribution functions from a global analysis of quantum chromodynamics, *Phys. Rev. D* **93**, 033006 (2016).
- [75] J. Butterworth *et al.*, PDF4LHC recommendations for LHC Run II, *J. Phys. G* **43**, 023001 (2016).
- [76] ATLAS Collaboration, Precision measurement and interpretation of inclusive W^+ , W^- and Z/γ^* production cross sections with the ATLAS detector, *Eur. Phys. J. C* **77**, 367 (2017).
- [77] M. Czakon and A. Mitov, Top++: A program for the calculation of the top-pair cross-section at hadron colliders, *Comput. Phys. Commun.* **185**, 2930 (2014).
- [78] M. Aliev, H. Lacker, U. Langenfeld, S. Moch, P. Uwer, and M. Wiedermann, HATHOR—Hadronic top and heavy quarks cross section calculator, *Comput. Phys. Commun.* **182**, 1034 (2011).
- [79] P. Kant, O. M. Kind, T. Kintscher, T. Lohse, T. Martini, S. Mölbitz, P. Rieck, and P. Uwer, HatHor for single top-quark production: Updated predictions and uncertainty estimates for single top-quark production in hadronic collisions, *Comput. Phys. Commun.* **191**, 74 (2015).
- [80] N. Kidonakis, Two-loop soft anomalous dimensions for single top quark associated production with a W^- or H^- , *Phys. Rev. D* **82**, 054018 (2010).
- [81] T. Gleisberg, S. Höche, F. Krauss, M. Schönherr, S. Schumann, F. Siegert, and J. Winter, Event generation with SHERPA 1.1, *J. High Energy Phys.* **02** (2009) 007.
- [82] J. M. Campbell, R. K. Ellis, and C. Williams, Vector boson pair production at the LHC, *J. High Energy Phys.* **07** (2011) 018.
- [83] ATLAS Collaboration, Measurements of the production cross section of a Z boson in association with jets in pp collisions at $\sqrt{s} = 13$ TeV with the ATLAS detector, *Eur. Phys. J. C* **77**, 361 (2017).
- [84] A. L. Read, Presentation of search results: The CL_S technique, *J. Phys. G* **28**, 2693 (2002).
- [85] G. Cowan, K. Cranmer, E. Gross, and O. Vitells, Asymptotic formulae for likelihood-based tests of new physics, *Eur. Phys. J. C* **71**, 1554 (2011); **73**, 2501(E) (2013).
- [86] G. Choudalakis and D. Casadei, Plotting the differences between data and expectation, *Eur. Phys. J. Plus* **127**, 25 (2012).
- [87] ATLAS Collaboration, ATLAS computing acknowledgements, Report No. ATL-SOFT-PUB-2023-001, 2023, <https://cds.cern.ch/record/2869272>.

G. Aad¹⁰⁰, B. Abbott¹¹⁷, D. C. Abbott¹⁰¹, A. Abed Abud³⁴, K. Abeling⁵³, D. K. Abhayasinghe⁹², S. H. Abidi²⁷, H. Abramowicz¹⁴⁸, H. Abreu¹⁴⁷, Y. Abulaiti⁵, A. C. Abusleme Hoffman^{134a}, B. S. Acharya^{66a,66b,b}, B. Achkar⁵³, L. Adam⁹⁸, C. Adam Bourdarios⁴, L. Adamczyk^{82a}, L. Adamek¹⁵², S. V. Addepalli²⁴, J. Adelman¹¹³, A. Adiguzel^{11c,c}, S. Adorni⁵⁴, T. Adye¹³¹, A. A. Affolder¹³³, Y. Afik¹⁴⁷, C. Agapopoulou⁶⁴, M. N. Agaras¹², J. Agarwala^{70a,70b}, A. Aggarwal¹¹¹, C. Agheorghiesei^{25c}, J. A. Aguilar-Saavedra^{127f,127a,d}, A. Ahmad³⁴

F. Ahmadov^{36,e} W. S. Ahmed¹⁰² X. Ai⁴⁶ G. Aielli^{73a,73b} I. Aizenberg¹⁶⁵ S. Akatsuka⁸⁴ M. Akbiyik⁹⁸
T. P. A. Åkesson⁹⁵ A. V. Akimov³⁵ K. Al Khoury³⁹ G. L. Alberghi^{21b} J. Albert¹⁶¹ P. Albicocco⁵¹
M. J. Alconada Verzini⁸⁷ S. Alderweireldt⁵⁰ M. Aleksa³⁴ I. N. Aleksandrov³⁶ C. Alexa^{25b} T. Alexopoulos⁹
A. Alfonsi¹¹² F. Alfonsi^{21b} M. Alhroob¹¹⁷ B. Ali¹²⁹ S. Ali¹⁴⁵ M. Aliev³⁵ G. Alimonti^{68a} C. Allaire³⁴
B. M. M. Allbrooke¹⁴³ P. P. Allport¹⁹ A. Aloisio^{69a,69b} F. Alonso⁸⁷ C. Alpigiani¹³⁵ E. Alunno Camelia^{73a,73b}
M. Alvarez Estevez⁹⁷ M. G. Alviggi^{69a,69b} Y. Amaral Coutinho^{79b} A. Ambler¹⁰² L. Ambroz¹²³ C. Amelung³⁴
D. Amidei¹⁰⁴ S. P. Amor Dos Santos^{127a} S. Amoroso⁴⁶ C. S. Amrouche⁵⁴ C. Anastopoulos¹³⁶ N. Andari¹³²
T. Andeen¹⁰ J. K. Anders¹⁸ S. Y. Andreato^{45a,45b} A. Andreatza^{68a,68b} S. Angelidakis⁸ A. Angerami³⁹
A. V. Anisenkov³⁵ A. Annovi^{71a} C. Antel⁵⁴ M. T. Anthony¹³⁶ E. Antipov¹¹⁸ M. Antonelli⁵¹
D. J. A. Antrim^{16a} F. Anulli^{72a} M. Aoki⁸⁰ J. A. Aparisi Pozo¹⁵⁹ M. A. Aparo¹⁴³ L. Aperio Bella⁴⁶
N. Aranzabal³⁴ V. Araujo Ferraz^{79a} C. Arcangeletti⁵¹ A. T. H. Arce⁴⁹ E. Arena⁸⁹ J-F. Arguin¹⁰⁶
S. Argyropoulos⁵² J.-H. Arling⁴⁶ A. J. Armbruster³⁴ A. Armstrong¹⁵⁶ O. Arnaez¹⁵² H. Arnold³⁴
Z. P. Arrubarrena Tame¹⁰⁷ G. Artoni¹²³ H. Asada¹⁰⁹ K. Asai¹¹⁵ S. Asai¹⁵⁰ N. A. Asbah⁵⁹
E. M. Asimakopoulou¹⁵⁷ L. Asquith¹⁴³ K. Assamagan²⁷ R. Astalos^{26a} R. J. Atkin^{31a} M. Atkinson¹⁵⁸
N. B. Atlay¹⁷ H. Atmani^{60b} P. A. Atmasiddha¹⁰⁴ K. Augsten¹²⁹ S. Auricchio^{69a,69b} V. A. Austrup¹⁶⁷
G. Avner¹⁴⁷ G. Avolio³⁴ M. K. Ayoub^{13c} G. Azuelos^{106,f} D. Babal^{26a} H. Bachacou¹³² K. Bachas¹⁴⁹
A. Bachi³² F. Backman^{45a,45b} A. Badea⁵⁹ P. Bagnaia^{72a,72b} H. Bahrasemani¹³⁹ A. J. Bailey¹⁵⁹ V. R. Bailey¹⁵⁸
J. T. Baines¹³¹ C. Bakalis⁹ O. K. Baker¹⁶⁸ P. J. Bakker¹¹² E. Bakos¹⁴ D. Bakshi Gupta⁷ S. Balaji¹⁴⁴
R. Balasubramanian¹¹² E. M. Baldin³⁵ P. Balek¹³⁰ E. Ballabene^{68a,68b} F. Balli¹³² W. K. Balunas¹²³ J. Balz⁹⁸
E. Banas⁸³ M. Bandieramonte¹²⁶ A. Bandyopadhyay¹⁷ S. Bansal²² L. Barak¹⁴⁸ E. L. Barberio¹⁰³
D. Barberis^{55b,55a} M. Barbero¹⁰⁰ G. Barbour⁹³ K. N. Barends^{31a} T. Barillari¹⁰⁸ M-S. Barisits³⁴ J. Barkeloo¹²⁰
T. Barklow¹⁴⁰ B. M. Barnett¹³¹ R. M. Barnett^{16a} A. Baroncelli^{60a} G. Barone²⁷ A. J. Barr¹²³
L. Barranco Navarro^{45a,45b} F. Barreiro⁹⁷ J. Barreiro Guimarães da Costa^{13a} U. Barron¹⁴⁸ S. Barsov³⁵
F. Bartels^{61a} R. Bartoldus¹⁴⁰ G. Bartolini¹⁰⁰ A. E. Barton⁸⁸ P. Bartos^{26a} A. Basalae⁴⁶ A. Basan⁹⁸
I. Bashta^{74a,74b} A. Bassalat^{64,g} M. J. Basso¹⁵² C. R. Basson⁹⁹ R. L. Bates⁵⁷ S. Batlamous^{33e} J. R. Batley³⁰
B. Batool¹³⁸ M. Battaglia¹³³ M. Bauge^{72a,72b} F. Bauer^{132,a} P. Bauer²² H. S. Bawa²⁹ A. Bayirli^{11c}
J. B. Beacham⁴⁹ T. Beau¹²⁴ P. H. Beauchemin¹⁵⁵ F. Becherer⁵² P. Bechtel²² H. P. Beck^{18,h} K. Becker¹⁶³
C. Becot⁴⁶ A. J. Beddall^{11a} V. A. Bednyakov³⁶ C. P. Bee¹⁴² T. A. Beermann¹⁶⁷ M. Begalli^{79b} M. Begel²⁷
A. Behera¹⁴² J. K. Behr⁴⁶ C. Beirao Da Cruz E Silva³⁴ J. F. Beirer^{53,34} F. Beisiegel²² M. Belfkir⁴ G. Bella¹⁴⁸
L. Bellagamba^{21b} A. Bellerive³² P. Bellos¹⁹ K. Beloborodov³⁵ K. Belotskiy³⁵ N. L. Belyaev³⁵
D. Benckekroun^{33a} Y. Benhammou¹⁴⁸ D. P. Benjamin²⁷ M. Benoit²⁷ J. R. Bensinger²⁴ S. Bentvelsen¹¹²
L. Beresford³⁴ M. Beretta⁵¹ D. Berge¹⁷ E. Bergeas Kuutmann¹⁵⁷ N. Berger⁴ B. Bergmann¹²⁹
L. J. Bergsten²⁴ J. Beringer^{16a} S. Berlendis⁶ G. Bernardi¹²⁴ C. Bernius¹⁴⁰ F. U. Bernlochner²² T. Berry⁹²
P. Berta¹³⁰ A. Berthold⁴⁸ I. A. Bertram⁸⁸ O. Bessidskaia Bylund¹⁶⁷ S. Bethke¹⁰⁸ A. Betti⁴² A. J. Bevan⁹¹
S. Bhatta¹⁴² D. S. Bhattacharya¹⁶² P. Bhattarai²⁴ V. S. Bhopatkar⁵ R. Bi¹²⁶ R. M. Bianchi¹²⁶ O. Biebel¹⁰⁷
R. Bielski¹²⁰ N. V. Biesuz^{71a,71b} M. Biglietti^{74a} T. R. V. Billoud¹²⁹ M. Bindi⁵³ A. Bingul^{11d} C. Bini^{72a,72b}
S. Biondi^{21b,21a} A. Biondini⁸⁹ C. J. Birch-sykes⁹⁹ G. A. Bird^{19,131} M. Birman¹⁶⁵ T. Bisanz³⁴ D. Biswas^{166,i}
A. Bitadze⁹⁹ C. Bittrich⁴⁸ K. Bjørke¹²² I. Bloch⁴⁶ C. Blocker²⁴ A. Blue⁵⁷ U. Blumenschein⁹¹
J. Blumenthal⁹⁸ G. J. Bobbink¹¹² V. S. Bobrovnikov³⁵ M. Boehler⁵² D. Bogavac¹² A. G. Bogdanchikov³⁵
C. Boehm^{45a} V. Boisvert⁹² P. Bokan⁴⁶ T. Bold^{82a} M. Bomben¹²⁴ M. Bona⁹¹ M. Boonekamp¹³²
C. D. Booth⁹² A. G. Borbély⁵⁷ H. M. Borecka-Bielska¹⁰⁶ L. S. Borgna⁹³ G. Borissov⁸⁸ D. Bortoletto¹²³
D. Boscherini^{21b} M. Bosman¹² J. D. Bossio Sola³⁴ K. Bouaouda^{33a} J. Boudreau¹²⁶ E. V. Bouhova-Thacker⁸⁸
D. Boumediene³⁸ R. Bouquet¹²⁴ A. Boveia¹¹⁶ J. Boyd³⁴ D. Boye²⁷ I. R. Boyko³⁶ A. J. Bozson⁹²
J. Bracinik¹⁹ N. Brahimi^{60d,60c} G. Brandt¹⁶⁷ O. Brandt³⁰ F. Braren⁴⁶ B. Brau¹⁰¹ J. E. Brau¹²⁰
W. D. Bredden Madden⁵⁷ K. Brendlinger⁴⁶ R. Brenner¹⁶⁵ L. Brenner³⁴ R. Brenner¹⁵⁷ S. Bressler¹⁶⁵
B. Brickwedde⁹⁸ D. L. Briglin¹⁹ D. Britton⁵⁷ D. Britzger¹⁰⁸ I. Brock²² R. Brock¹⁰⁵ G. Brooijmans³⁹
W. K. Brooks^{134e} E. Brost²⁷ P. A. Bruckman de Renstrom⁸³ B. Brüers⁴⁶ D. Bruncko^{26b,a} A. Bruni^{21b}
G. Bruni^{21b} M. Bruschi^{21b} N. Bruscino^{72a,72b} L. Bryngemark¹⁴⁰ T. Buanes¹⁵ Q. Buat¹⁴² P. Buchholz¹³⁸
A. G. Buckley⁵⁷ I. A. Budagov^{36,a} M. K. Bugge¹²² O. Bulekov³⁵ B. A. Bullard⁵⁹ T. J. Burch¹¹³ S. Burdini⁸⁹

C. D. Burgard⁴⁶ A. M. Burger¹¹⁸ B. Burghgrave⁷ J. T. P. Burr⁴⁶ C. D. Burton¹⁰ J. C. Burzynski¹⁰¹
V. Büscher⁹⁸ P. J. Bussey⁵⁷ J. M. Butler²³ C. M. Buttar⁵⁷ J. M. Butterworth⁹³ W. Buttinger¹³¹
C. J. Buxo Vazquez¹⁰⁵ A. R. Buzykaev³⁵ G. Cabras^{21b} S. Cabrera Urbán¹⁵⁹ D. Caforio⁵⁶ H. Cai¹²⁶
V. M. M. Cairo¹⁴⁰ O. Cakir^{3a} N. Calace³⁴ P. Calafiura^{16a} G. Calderini¹²⁴ P. Calfayan⁶⁵ G. Callea⁵⁷
L. P. Caloba^{79b} S. Calvente Lopez⁹⁷ D. Calvet³⁸ S. Calvet³⁸ T. P. Calvet¹⁰⁰ M. Calvetti^{71a,71b}
R. Camacho Toro¹²⁴ S. Camarda³⁴ D. Camarero Munoz⁹⁷ P. Camarri^{73a,73b} M. T. Camerlingo^{74a,74b}
D. Cameron¹²² C. Camincher¹⁶¹ M. Campanelli⁹³ A. Camplani⁴⁰ V. Canale^{69a,69b} A. Canesse¹⁰²
M. Cano Bret⁷⁷ J. Cantero¹¹⁸ Y. Cao¹⁵⁸ F. Capocasa²⁴ M. Capua^{41b,41a} A. Carbone^{68a,68b} R. Cardarelli^{73a}
J. C. J. Cardenas⁷ F. Cardillo¹⁵⁹ T. Carli³⁴ G. Carlino^{69a} B. T. Carlson¹²⁶ E. M. Carlson^{161,153a}
L. Carminati^{68a,68b} M. Carnesale^{72a,72b} R. M. D. Carney¹⁴⁰ S. Caron¹¹¹ E. Carquin^{134e} S. Carrá⁴⁶
G. Carratta^{21b,21a} J. W. S. Carter¹⁵² T. M. Carter⁵⁰ D. Casadei^{31c} M. P. Casado^{12j} A. F. Casha¹⁵²
E. G. Castiglia¹⁶⁸ F. L. Castillo^{61a} L. Castillo Garcia¹² V. Castillo Gimenez¹⁵⁹ N. F. Castro^{127a,127e}
A. Catinaccio³⁴ J. R. Catmore¹²² A. Cattai³⁴ V. Cavaliere²⁷ N. Cavalli^{21b,21a} V. Cavasinni^{71a,71b} E. Celebi^{11b}
F. Celli¹²³ M. S. Centonze^{67a,67b} K. Cerny¹¹⁹ A. S. Cerqueira^{79a} A. Cerri¹⁴³ L. Cerrito^{73a,73b} F. Cerutti^{16a}
A. Cervelli^{21b} S. A. Cetin^{11b} Z. Chadi^{33a} D. Chakraborty¹¹³ M. Chala^{127f} J. Chan¹⁶⁶ W. S. Chan¹¹²
W. Y. Chan⁸⁹ J. D. Chapman³⁰ B. Chargeishvili^{146b} D. G. Charlton¹⁹ T. P. Charman⁹¹ M. Chatterjee¹⁸
S. Chekanov⁵ S. V. Chekulaev^{153a} G. A. Chelkov^{36,k} A. Chen¹⁰⁴ B. Chen¹⁴⁸ C. Chen^{60a} C. H. Chen⁷⁸
H. Chen^{13c} H. Chen²⁷ J. Chen^{60c} J. Chen²⁴ S. Chen¹²⁵ S. J. Chen^{13c} X. Chen^{60c} X. Chen^{13b,1} Y. Chen^{60a}
Y-H. Chen⁴⁶ C. L. Cheng¹⁶⁶ H. C. Cheng^{62a} A. Cheplakov³⁶ E. Cheremushkina⁴⁶ E. Cherepanova³⁶
R. Cherkaoui El Moursli^{33e} E. Cheu⁶ K. Cheung⁶³ L. Chevalier¹³² V. Chiarella⁵¹ G. Chiarelli^{71a}
G. Chiodini^{67a} A. S. Chisholm¹⁹ A. Chitan^{25b} Y. H. Chiu¹⁶¹ M. V. Chizhov^{36,m} K. Choi¹⁰
A. R. Chomont^{72a,72b} Y. Chou¹⁰¹ E. Y. S. Chow¹¹² L. D. Christopher^{31f} M. C. Chu^{62a} X. Chu^{13a,13d}
J. Chudoba¹²⁸ J. J. Chwastowski⁸³ D. Cieri¹⁰⁸ K. M. Ciesla⁸³ V. Cindro⁹⁰ I. A. Cioară^{25b} A. Ciocio^{16a}
F. Ciroto^{69a,69b} Z. H. Citron^{165,n} M. Citterio^{68a} D. A. Ciubotaru^{25b} B. M. Ciungu¹⁵² A. Clark⁵⁴ P. J. Clark⁵⁰
J. M. Clavijo Columbie⁴⁶ S. E. Clawson⁹⁹ C. Clement^{45a,45b} Y. Coadou¹⁰⁰ M. Cobal^{66a,66c} A. Coccaro^{55b}
J. Cochran⁷⁸ R. F. Coelho Barrue^{127a} R. Coelho Lopes De Sa¹⁰¹ S. Coelli^{68a} H. Cohen¹⁴⁸ A. E. C. Coimbra³⁴
B. Cole³⁹ J. Collot⁵⁸ P. Conde Muiño^{127a,127h} S. H. Connell^{31c} I. A. Connelly⁵⁷ E. I. Conroy¹²³
F. Conventi^{69a,o} H. G. Cooke¹⁹ A. M. Cooper-Sarkar¹²³ F. Cormier¹⁶⁰ L. D. Corpe³⁴ M. Corradi^{72a,72b}
E. E. Corrigan⁹⁵ F. Corriveau^{102,p} M. J. Costa¹⁵⁹ F. Costanza⁴ D. Costanzo¹³⁶ B. M. Cote¹¹⁶ G. Cowan⁹²
J. W. Cowley³⁰ K. Cranmer¹¹⁴ S. Crépe-Renaudin⁵⁸ F. Crescioli¹²⁴ M. Cristinziani¹³⁸ M. Cristoforetti^{75a,75b,q}
V. Croft¹⁵⁵ G. Crosetti^{41b,41a} A. Cueto³⁴ T. Cuhadar Donszelmann¹⁵⁶ H. Cui^{13a,13d} A. R. Cukierman¹⁴⁰
W. R. Cunningham⁵⁷ P. Czodrowski³⁴ M. M. Czurylo^{61b} M. J. Da Cunha Sargedas De Sousa^{60a}
J. V. Da Fonseca Pinto^{79b} C. Da Via⁹⁹ W. Dabrowski^{82a} T. Dado⁴⁷ S. Dahbi^{31f} T. Dai¹⁰⁴ C. Dallapiccola¹⁰¹
M. Dam⁴⁰ G. D'amen²⁷ V. D'Amico^{74a,74b} J. Damp⁹⁸ J. R. Dandoy¹²⁵ M. F. Daneri²⁸ M. Danninger¹³⁹
V. Dao³⁴ G. Darbo^{55b} S. Darmora⁵ A. Dattagupta¹²⁰ S. D'Auria^{68a,68b} C. David^{153b} T. Davidek¹³⁰
D. R. Davis⁴⁹ B. Davis-Purcell³² I. Dawson⁹¹ K. De⁷ R. De Asmundis^{69a} M. De Beurs¹¹² S. De Castro^{21b,21a}
N. De Groot¹¹¹ P. de Jong¹¹² H. De la Torre¹⁰⁵ A. De Maria^{13c} D. De Pedis^{72a} A. De Salvo^{72a}
U. De Sanctis^{73a,73b} M. De Santis^{73a,73b} A. De Santo¹⁴³ J. B. De Vivie De Regie⁵⁸ D. V. Dedovich³⁶ J. Degens¹¹²
A. M. Deiana⁴² J. Del Peso⁹⁷ Y. Delabat Diaz⁴⁶ F. Deliot¹³² C. M. Delitzsch⁶ M. Della Pietra^{69a,69b}
D. Della Volpe⁵⁴ A. Dell'Acqua³⁴ L. Dell'Asta^{68a,68b} M. Delmastro⁴ P. A. Delsart⁵⁸ S. Demers¹⁶⁸
M. Demichev³⁶ S. P. Denisov³⁵ L. D'Eramo¹¹³ D. Derendarz⁸³ J. E. Derkaoui^{33d} F. Derue¹²⁴ P. Dervan⁸⁹
K. Desch²² K. Dette¹⁵² C. Deutsch²² P. O. Deviveiros³⁴ F. A. Di Bello^{72a,72b} A. Di Ciaccio^{73a,73b}
L. Di Ciaccio⁴ C. Di Donato^{69a,69b} A. Di Girolamo³⁴ G. Di Gregorio^{71a,71b} A. Di Luca^{75a,75b} B. Di Micco^{74a,74b}
R. Di Nardo^{74a,74b} C. Diaconu¹⁰⁰ F. A. Dias¹¹² T. Dias Do Vale^{127a} M. A. Diaz^{134a,134b} F. G. Diaz Capriles²²
J. Dickinson^{16a} M. Didenko¹⁵⁹ E. B. Diehl¹⁰⁴ J. Dietrich¹⁷ S. Díez Cornell⁴⁶ C. Diez Pardos¹³⁸
A. Dimitrievska^{16a} W. Ding^{13b} J. Dingfelder²² I-M. Dinu^{25b} S. J. Dittmeier^{61b} F. Dittus³⁴ F. Djama¹⁰⁰
T. Djobava^{146b} J. I. Djuvsland¹⁵ M. A. B. Do Vale^{79c} D. Dodsworth²⁴ C. Doglioni⁹⁵ J. Dolejsi¹³⁰
Z. Dolezal¹³⁰ M. Donadelli^{79d} B. Dong^{60c} J. Donini³⁸ A. D'Onofrio^{13c} M. D'Onofrio⁸⁹ J. Dopke¹³¹
A. Doria^{69a} M. T. Dova⁸⁷ A. T. Doyle⁵⁷ E. Drechsler¹³⁹ E. Dreyer¹³⁹ T. Dreyer⁵³ A. S. Drobac¹⁵⁵

D. Du^{60b} T. A. du Pree¹¹² F. Dubinin³⁵ M. Dubovsky^{26a} A. Dubreuil⁵⁴ E. Duchovni¹⁶⁵ G. Duckeck¹⁰⁷
 O. A. Ducu^{34,25b} D. Duda¹⁰⁸ A. Dudarev³⁴ M. D'uffizi⁹⁹ L. Dufлот⁶⁴ M. Dührssen³⁴ C. Dülsen¹⁶⁷
 A. E. Dumitriu^{25b} M. Dunford^{61a} S. Dungs⁴⁷ K. Dunne^{45a,45b} A. Duperrin¹⁰⁰ H. Duran Yildiz^{3a} M. Düren⁵⁶
 A. Durglishvili^{146b} B. Dutta⁴⁶ B. L. Dwyer¹¹³ G. I. Dyckes¹²⁵ M. Dyndal^{82a} S. Dysch⁹⁹ B. S. Dziedzic⁸³
 B. Eckerova^{26a} M. G. Eggleston⁴⁹ E. Egidio Purcino De Souza^{79b} L. F. Ehrke⁵⁴ T. Eifert⁷ G. Eigen¹⁵
 K. Einsweiler^{16a} T. Ekelof¹⁵⁷ Y. El Ghazali^{33b} H. El Jarrari^{33e} A. El Moussaouy^{33a} V. Ellajosyula¹⁵⁷
 M. Ellert¹⁵⁷ F. Ellinghaus¹⁶⁷ A. A. Elliot⁹¹ N. Ellis³⁴ J. Elmsheuser²⁷ M. Elsing³⁴ D. Emeliyanov¹³¹
 A. Emerman³⁹ Y. Enari¹⁵⁰ J. Erdmann⁴⁷ A. Ereditato¹⁸ P. A. Erland⁸³ M. Errenst¹⁶⁷ M. Escalier⁶⁴
 C. Escobar¹⁵⁹ O. Estrada Pastor¹⁵⁹ E. Etzion¹⁴⁸ G. Evans^{127a} H. Evans⁶⁵ M. O. Evans¹⁴³ A. Ezhilov³⁵
 F. Fabbri⁵⁷ L. Fabbri^{21b,21a} V. Fabiani¹¹¹ G. Facini¹⁶³ V. Fadeyev¹³³ R. M. Fakhruddinov³⁵ S. Falciano^{72a}
 P. J. Falke²² S. Falke³⁴ J. Faltova¹³⁰ Y. Fan^{13a} Y. Fang^{13a} Y. Fang^{13a,13d} G. Fanourakis⁴⁴ M. Fanti^{68a,68b}
 M. Faraj^{60c} A. Farbin⁷ A. Farilla^{74a} E. M. Farina^{70a,70b} T. Farooque¹⁰⁵ S. M. Farrington⁵⁰ P. Farthouat³⁴
 F. Fassi^{33e} D. Fassouliotis⁸ M. Fauci Giannelli^{73a,73b} W. J. Fawcett³⁰ L. Fayard⁶⁴ O. L. Fedin^{35,k}
 M. Feickert¹⁵⁸ L. Feligioni¹⁰⁰ A. Fell¹³⁶ C. Feng^{60b} M. Feng^{13b} M. J. Fenton¹⁵⁶ A. B. Fenyuk³⁵
 S. W. Ferguson⁴³ J. Ferrando⁴⁶ A. Ferrari¹⁵⁷ P. Ferrari¹¹² R. Ferrari^{70a} D. Ferrere⁵⁴ C. Ferretti¹⁰⁴
 F. Fiedler⁹⁸ A. Filipčič⁹⁰ F. Filthaut¹¹¹ M. C. N. Fiolhais^{127a,127c,r} L. Fiorini¹⁵⁹ F. Fischer¹³⁸ W. C. Fisher¹⁰⁵
 T. Fitschen¹⁹ I. Fleck¹³⁸ P. Fleischmann¹⁰⁴ T. Flick¹⁶⁷ B. M. Flierl¹⁰⁷ L. Flores¹²⁵ L. R. Flores Castillo^{62a}
 F. M. Follega^{75a,75b} N. Fomin¹⁵ J. H. Foo¹⁵² B. C. Forland⁶⁵ A. Formica¹³² F. A. Förster¹² A. C. Forti⁹⁹
 E. Fortin¹⁰⁰ M. G. Foti¹²³ D. Fournier⁶⁴ H. Fox⁸⁸ P. Francavilla^{71a,71b} S. Francescato⁵⁹ M. Franchini^{21b,21a}
 S. Franchino^{61a} D. Francis³⁴ L. Franco⁴ L. Franconi¹⁸ M. Franklin⁵⁹ G. Frattari^{72a,72b} A. C. Freegard⁹¹
 P. M. Freeman¹⁹ W. S. Freund^{79b} E. M. Freundlich⁴⁷ D. Froidevaux³⁴ J. A. Frost¹²³ Y. Fu^{60a} M. Fujimoto¹¹⁵
 E. Fullana Torregrosa^{159,a} J. Fuster¹⁵⁹ A. Gabrielli^{21b,21a} A. Gabrielli³⁴ P. Gadow⁴⁶ G. Gagliardi^{55b,55a}
 L. G. Gagnon^{16a} G. E. Gallardo¹²³ E. J. Gallas¹²³ B. J. Gallop¹³¹ R. Gamboa Goni⁹¹ K. K. Gan¹¹⁶
 S. Ganguly¹⁶⁵ J. Gao^{60a} Y. Gao⁵⁰ Y. S. Gao^{29,s} F. M. Garay Walls^{134a} C. García¹⁵⁹ J. E. García Navarro¹⁵⁹
 J. A. García Pascual^{13a} M. Garcia-Sciveres^{16a} R. W. Gardner³⁷ D. Garg⁷⁷ S. Gargiulo⁵² C. A. Garner¹⁵²
 V. Garonne¹²² S. J. Gasiorowski¹³⁵ P. Gaspar^{79b} G. Gaudio^{70a} P. Gauzzi^{72a,72b} I. L. Gavrilenko³⁵
 A. Gavriilyuk³⁵ C. Gay¹⁶⁰ G. Gaycken⁴⁶ E. N. Gazis⁹ A. A. Geanta^{25b} C. M. Gee¹³³ C. N. P. Gee¹³¹
 J. Geisen⁹⁵ M. Geisen⁹⁸ C. Gemme^{55b} M. H. Genest⁵⁸ S. Gentile^{72a,72b} S. George⁹² W. F. George¹⁹
 T. Gerialis⁴⁴ L. O. Gerlach⁵³ P. Gessinger-Befurt³⁴ M. Ghasemi Bostanabad¹⁶¹ M. Ghneimat¹³⁸ A. Ghosh¹⁵⁶
 A. Ghosh⁷⁷ B. Giacobbe^{21b} S. Giagu^{72a,72b} N. Giangiacomi¹⁵² P. Giannetti^{71a} A. Giannini^{69a,69b}
 S. M. Gibson⁹² M. Gignac¹³³ D. T. Gil^{82b} B. J. Gilbert³⁹ D. Gillberg³² G. Gilles¹¹² N. E. K. Gillwald⁴⁶
 D. M. Gingrich^{2,f} M. P. Giordani^{66a,66c} P. F. Giraud¹³² G. Giugliarelli^{66a,66c} D. Giugni^{68a} F. Giuli^{73a,73b}
 I. Gkiyalas^{8,t} P. Gkoutoumis⁹ L. K. Gladilin³⁵ C. Glasman⁹⁷ G. R. Gledhill¹²⁰ M. Glisic¹²⁰ I. Gnesi^{41b,u}
 M. Goblirsch-Kolb²⁴ D. Godin¹⁰⁶ S. Goldfarb¹⁰³ T. Golling⁵⁴ D. Golubkov³⁵ J. P. Gombas¹⁰⁵
 A. Gomes^{127a,127b} R. Goncalves Gama⁵³ R. Gonçalves^{127a,127c} G. Gonella¹²⁰ L. Gonella¹⁹ A. Gongadze³⁶
 F. Gonnella¹⁹ J. L. Gonski³⁹ R. Y. González Andana^{134a} S. González de la Hoz¹⁵⁹ S. Gonzalez Fernandez¹²
 R. Gonzalez Lopez⁸⁹ C. Gonzalez Renteria^{16a} R. Gonzalez Suarez¹⁵⁷ S. Gonzalez-Sevilla⁵⁴
 G. R. Gonzalvo Rodriguez¹⁵⁹ L. Goossens³⁴ N. A. Gorasia¹⁹ P. A. Gorbounov³⁵ B. Gorini³⁴ E. Gorini^{67a,67b}
 A. Gorišek⁹⁰ A. T. Goshaw⁴⁹ M. I. Gostkin³⁶ C. A. Gottardo¹¹¹ M. Gouighri^{33b} V. Goumarre⁴⁶
 A. G. Goussiou¹³⁵ N. Govender^{31c} C. Goy⁴ I. Grabowska-Bold^{82a} K. Graham³² E. Gramstad¹²²
 S. Grancagnolo¹⁷ M. Grandi¹⁴³ V. Gratchev^{35,a} P. M. Gravila^{25f} F. G. Gravili^{67a,67b} H. M. Gray^{16a} C. Grefe²²
 I. M. Gregor⁴⁶ P. Grenier¹⁴⁰ K. Grevtsov⁴⁶ C. Grieco¹² N. A. Grieser¹¹⁷ A. A. Grillo¹³³ K. Grimm^{29,v}
 S. Grinstein^{12,w} J.-F. Grivaz⁶⁴ S. Groh⁹⁸ E. Gross¹⁶⁵ J. Grosse-Knetter⁵³ C. Grud¹⁰⁴ A. Grummer¹¹⁰
 J. C. Grundy¹²³ L. Guan¹⁰⁴ W. Guan¹⁶⁶ C. Gubbels¹⁶⁰ J. Guenther³⁴ J. G. R. Guerrero Rojas¹⁵⁹
 F. Guescini¹⁰⁸ R. Gugel⁹⁸ A. Guida⁴⁶ T. Guillemin⁴ S. Guindon³⁴ J. Guo^{60c} L. Guo⁶⁴ Y. Guo¹⁰⁴
 R. Gupta⁴⁶ S. Gurbuz²² G. Gustavino¹¹⁷ M. Guth⁵⁴ P. Gutierrez¹¹⁷ L. F. Gutierrez Zagazeta¹²⁵
 C. Gutsche⁹³ C. Guyot¹³² C. Gwenlan¹²³ C. B. Gwilliam⁸⁹ E. S. Haaland¹²² A. Haas¹¹⁴ M. Habedank¹⁷
 C. Haber^{16a} H. K. Hadavand⁷ A. Hadeef⁹⁸ S. Hadzic¹⁰⁸ M. Haleem¹⁶² J. Haley¹¹⁸ J. J. Hall¹³⁶
 G. Halladjian¹⁰⁵ G. D. Hallowell¹⁰⁰ L. Halser¹⁸ K. Hamano¹⁶¹ M. Hamer²² G. N. Hamity⁵⁰ K. Han^{60a}

L. Han^{13c}, L. Han^{60a}, S. Han^{16a}, Y. F. Han¹⁵², K. Hanagaki⁸⁰, M. Hance¹³³, M. D. Hank³⁷, R. Hankache⁹⁹,
 E. Hansen⁹⁵, J. B. Hansen⁴⁰, J. D. Hansen⁴⁰, M. C. Hansen²², P. H. Hansen⁴⁰, K. Hara¹⁵⁴, T. Harenberg¹⁶⁷,
 S. Harkusha³⁵, Y. T. Harris¹²³, P. F. Harrison¹⁶³, N. M. Hartman¹⁴⁰, N. M. Hartmann¹⁰⁷, Y. Hasegawa¹³⁷,
 A. Hasib⁵⁰, S. Hassani¹³², S. Haug¹⁸, R. Hauser¹⁰⁵, M. Havranek¹²⁹, C. M. Hawkes¹⁹, R. J. Hawkings³⁴,
 S. Hayashida¹⁰⁹, D. Hayden¹⁰⁵, C. Hayes¹⁰⁴, R. L. Hayes¹⁶⁰, C. P. Hays¹²³, J. M. Hays⁹¹, H. S. Hayward⁸⁹,
 S. J. Haywood¹³¹, F. He^{60a}, Y. He¹⁵¹, Y. He¹²⁴, M. P. Heath⁵⁰, V. Hedberg⁹⁵, A. L. Heggelund¹²²,
 N. D. Hehir^{91,a}, C. Heidegger⁵², K. K. Heidegger⁵², W. D. Heidorn⁷⁸, J. Heilman³², S. Heim⁴⁶, T. Heim^{16a},
 B. Heinemann^{46,x}, J. G. Heinlein¹²⁵, J. J. Heinrich¹²⁰, L. Heinrich³⁴, J. Hejbal¹²⁸, L. Helary⁴⁶, A. Held¹¹⁴,
 S. Hellesund¹²², C. M. Helling¹³³, S. Hellman^{45a,45b}, C. Helsens³⁴, R. C. W. Henderson⁸⁸, L. Henkelmann³⁰,
 A. M. Henriques Correia³⁴, H. Herde¹⁴⁰, Y. Hernández Jiménez¹⁴², H. Herr⁹⁸, M. G. Herrmann¹⁰⁷, T. Herrmann⁴⁸,
 G. Herten⁵², R. Hertenberger¹⁰⁷, L. Hervas³⁴, N. P. Hessey^{153a}, H. Hibi⁸¹, S. Higashino⁸⁰,
 E. Higón-Rodríguez¹⁵⁹, K. K. Hill²⁷, K. H. Hiller⁴⁶, S. J. Hillier¹⁹, M. Hils⁴⁸, I. Hinchliffe^{16a}, F. Hinterkeuser²²,
 M. Hirose¹²¹, S. Hirose¹⁵⁴, D. Hirschbuehl¹⁶⁷, B. Hiti⁹⁰, O. Hladik¹²⁸, J. Hobbs¹⁴², R. Hobincu^{25e}, N. Hod¹⁶⁵,
 M. C. Hodgkinson¹³⁶, B. H. Hodgkinson³⁰, A. Hoecker³⁴, J. Hofer⁴⁶, D. Hohn⁵², T. Holm²², T. R. Holmes³⁷,
 M. Holzbock¹⁰⁸, L. B. A. H. Hommels³⁰, B. P. Honan⁹⁹, J. Hong^{60c}, T. M. Hong¹²⁶, J. C. Honig⁵², A. Hönle¹⁰⁸,
 B. H. Hooberman¹⁵⁸, W. H. Hopkins⁵, Y. Horii¹⁰⁹, L. A. Horyn³⁷, S. Hou¹⁴⁵, J. Howarth⁵⁷, J. Hoya⁸⁷,
 M. Hrabovsky¹¹⁹, A. Hrynevich³⁵, T. Hryn'ova⁴, P. J. Hsu⁶³, S.-C. Hsu¹³⁵, Q. Hu³⁹, S. Hu^{60c}, Y. F. Hu^{13a,13d,y},
 D. P. Huang⁹³, X. Huang^{13c}, Y. Huang^{60a}, Y. Huang^{13a}, Z. Hubacek¹²⁹, F. Hubaut¹⁰⁰, M. Huebner²²,
 F. Huegging²², T. B. Huffman¹²³, M. Huhtinen³⁴, R. Hulsken⁵⁸, N. Huseynov^{36,e}, J. Huston¹⁰⁵, J. Huth⁵⁹,
 R. Hyneman¹⁴⁰, S. Hyrych^{26a}, G. Iacobucci⁵⁴, G. Iakovidis²⁷, I. Ibragimov¹³⁸, L. Iconomidou-Fayard⁶⁴,
 P. Inengo³⁴, R. Iguchi¹⁵⁰, T. Iizawa⁵⁴, Y. Ikegami⁸⁰, A. Ilg¹⁸, N. Ilic¹⁵², H. Imam^{33a},
 T. Ingebretsen Carlson^{45a,45b}, G. Introzzi^{70a,70b}, M. Iodice^{74a}, V. Ippolito^{72a,72b}, M. Ishino¹⁵⁰, W. Islam¹¹⁸,
 C. Issever^{17,46}, S. Istin^{11c,z}, J. M. Iturbe Ponce^{62a}, R. Iuppa^{75a,75b}, A. Ivina¹⁶⁵, J. M. Izen⁴³, V. Izzo^{69a},
 P. Jacka¹²⁸, P. Jackson¹, R. M. Jacobs⁴⁶, B. P. Jaeger¹³⁹, C. S. Jagfeld¹⁰⁷, G. Jäkel¹⁶⁷, K. Jakobs⁵²,
 T. Jakoubek¹⁶⁵, J. Jamieson⁵⁷, K. W. Janas^{82a}, G. Jarlskog⁹⁵, A. E. Jaspán⁸⁹, N. Javadov^{36,e}, T. Javůrek³⁴,
 M. Javurkova¹⁰¹, F. Jeanneau¹³², L. Jeanty¹²⁰, J. Jejelava^{146a,aa}, P. Jenni^{52,bb}, S. Jézéquel⁴, J. Jia¹⁴², Z. Jia^{13c},
 Y. Jiang^{60a}, S. Jiggins⁵², J. Jimenez Pena¹⁰⁸, S. Jin^{13c}, A. Jinaru^{25b}, O. Jinnouchi¹⁵¹, H. Jivan^{31f}, P. Johansson¹³⁶,
 K. A. Johns⁶, C. A. Johnson⁶⁵, D. M. Jones³⁰, E. Jones¹⁶³, R. W. L. Jones⁸⁸, T. J. Jones⁸⁹, J. Jovicevic⁵³,
 X. Ju^{16a}, J. J. Junggeburth³⁴, A. Juste Rozas^{12,w}, S. Kabana^{134d}, A. Kaczmarska⁸³, M. Kado^{72a,72b}, H. Kagan¹¹⁶,
 M. Kagan¹⁴⁰, A. Kahn³⁹, C. Kahra⁹⁸, T. Kaji¹⁶⁴, E. Kajomovitz¹⁴⁷, C. W. Kalderon²⁷, A. Kamenshchikov³⁵,
 M. Kaneda¹⁵⁰, N. J. Kang¹³³, S. Kang⁷⁸, Y. Kano¹⁰⁹, J. Kanzaki⁸⁰, D. Kar^{31f}, K. Karava¹²³, M. J. Kareem^{153b},
 I. Karkanas¹⁴⁹, S. N. Karpov³⁶, Z. M. Karpova³⁶, V. Kartvelishvili⁸⁸, A. N. Karyukhin³⁵, E. Kasimi¹⁴⁹,
 C. Kato^{60d}, J. Katzy⁴⁶, K. Kawade¹³⁷, K. Kawagoe⁸⁶, T. Kawaguchi¹⁰⁹, T. Kawamoto¹³², G. Kawamura,
 E. F. Kay¹⁶¹, F. I. Kaya¹⁵⁵, S. Kazakos¹², V. F. Kazanin³⁵, Y. Ke¹⁴², J. M. Keaveney^{31a}, R. Keeler¹⁶¹,
 J. S. Keller³², D. Kelsey¹⁴³, J. J. Kempster¹⁹, J. Kendrick¹⁹, K. E. Kennedy³⁹, O. Kepka¹²⁸, S. Kersten¹⁶⁷,
 B. P. Kerševan⁹⁰, S. Ketabchi Haghighat¹⁵², M. Khandoga¹²⁴, A. Khanov¹¹⁸, A. G. Kharlamov³⁵,
 T. Kharlamova³⁵, E. E. Khoda¹³⁵, T. J. Khoo¹⁷, G. Khoriauli¹⁶², J. Khubua^{146b}, S. Kido⁸¹, M. Kiehn³⁴,
 A. Kilgallon¹²⁰, E. Kim¹⁵¹, Y. K. Kim³⁷, N. Kimura⁹³, A. Kirchhoff⁵³, D. Kirchmeier⁴⁸, C. Kirfel²², J. Kirk¹³¹,
 A. E. Kiryunin¹⁰⁸, T. Kishimoto¹⁵⁰, D. P. Kisiuk¹⁵², V. Kitali⁴⁶, C. Kitsaki⁹, O. Kivernyk²²,
 T. Klapdor-Kleingrothaus⁵², M. Klassen^{61a}, C. Klein³², L. Klein¹⁶², M. H. Klein¹⁰⁴, M. Klein⁸⁹, U. Klein⁸⁹,
 P. Klimek³⁴, A. Klimentov²⁷, F. Klimpel³⁴, T. Klingl²², T. Klioutchnikova³⁴, F. F. Klitzner¹⁰⁷, P. Kluit¹¹²,
 S. Kluth¹⁰⁸, E. Kneringer⁷⁶, T. M. Knight¹⁵², A. Knue⁵², D. Kobayashi⁸⁶, M. Kobel⁴⁸, M. Kocian¹⁴⁰,
 T. Kodama¹⁵⁰, P. Kodyš¹³⁰, D. M. Koeck¹⁴³, P. T. Koenig²², T. Koffas³², N. M. Köhler³⁴, M. Kolb¹³²,
 I. Koletsou⁴, T. Komarek¹¹⁹, K. Köneke⁵², A. X. Y. Kong¹, T. Kono¹¹⁵, V. Konstantinides⁹³, N. Konstantinidis⁹³,
 B. Konya⁹⁵, R. Kopeliansky⁶⁵, S. Koperny^{82a}, K. Korcyl⁸³, K. Kordas¹⁴⁹, G. Koren¹⁴⁸, A. Korn⁹³, S. Korn⁵³,
 I. Korolkov¹², E. V. Korolkova¹³⁶, N. Korotkova³⁵, B. Kortman¹¹², O. Kortner¹⁰⁸, S. Kortner¹⁰⁸,
 W. H. Kostecka¹¹³, V. V. Kostyukhin^{136,35}, A. Kotskechagia⁶⁴, A. Kotwal⁴⁹, A. Koulouris³⁴,
 A. Kourkoumeli-Charalampidi^{70a,70b}, C. Kourkoumelis⁸, E. Kourlitis⁵, O. Kovanda¹⁴³, R. Kowalewski¹⁶¹,
 W. Kozanecki¹³², A. S. Kozhin³⁵, V. A. Kramarenko³⁵, G. Kramberger⁹⁰, D. Krasnopevtsev^{60a}, M. W. Krasny¹²⁴

A. Krasznahorkay³⁴ J. A. Kremer⁹⁸ J. Kretzschmar⁸⁹ K. Kreul¹⁷ P. Krieger¹⁵² F. Krieter¹⁰⁷
S. Krishnamurthy¹⁰¹ A. Krishnan^{61b} M. Krivos¹³⁰ K. Krizka^{16a} K. Kroeninger⁴⁷ H. Kroha¹⁰⁸ J. Kroll¹²⁸
J. Kroll¹²⁵ K. S. Krowpman¹⁰⁵ U. Kruchonak³⁶ H. Krüger²² N. Krumnack⁷⁸ M. C. Kruse⁴⁹ J. A. Krzysiak⁸³
A. Kubota¹⁵¹ O. Kuchinskaia³⁵ S. Kuday^{3b} D. Kuechler⁴⁶ J. T. Kuechler⁴⁶ S. Kuehn³⁴ T. Kuhl⁴⁶
V. Kukhtin³⁶ Y. Kulchitsky^{35,k} S. Kuleshov^{134c} M. Kumar^{31f} N. Kumari¹⁰⁰ M. Kuna⁵⁸ A. Kupco¹²⁸
T. Kupfer⁴⁷ O. Kuprash⁵² H. Kurashige⁸¹ L. L. Kurchaninov^{153a} Y. A. Kurochkin³⁵ A. Kurova³⁵
M. G. Kurth^{13a,13d} E. S. Kuwertz³⁴ M. Kuze¹⁵¹ A. K. Kvam¹³⁵ J. Kvita¹¹⁹ T. Kwan¹⁰² K. W. Kwok^{62a}
C. Lacasta¹⁵⁹ F. Lacava^{72a,72b} H. Lacker¹⁷ D. Lacour¹²⁴ N. N. Lad⁹³ E. Ladygin³⁶ R. Lafaye⁴
B. Laforge¹²⁴ T. Lagouri^{134d} S. Lai⁵³ I. K. Lakomic^{82a} N. Lalloue⁵⁸ J. E. Lambert¹¹⁷ S. Lammers⁶⁵
W. Lampl⁶ C. Lampoudis¹⁴⁹ E. Lançon²⁷ U. Landgraf⁵² M. P. J. Landon⁹¹ V. S. Lang⁵² J. C. Lange⁵³
R. J. Langenberg¹⁰¹ A. J. Lankford¹⁵⁶ F. Lanni²⁷ K. Lantzsch²² A. Lanza^{70a} A. Lapertosa^{55b,55a}
J. F. Laporte¹³² T. Lari^{68a} F. Lasagni Manghi^{21b} M. Lassnig³⁴ V. Latonova¹²⁸ T. S. Lau^{62a} A. Laudrain⁹⁸
A. Laurier³² M. Lavorgna^{69a,69b} S. D. Lawlor⁹² Z. Lawrence⁹⁹ M. Lazzaroni^{68a,68b} B. Le⁹⁹ B. Leban⁹⁰
A. Lebedev⁷⁸ M. LeBlanc³⁴ T. LeCompte⁵ F. Ledroit-Guillon⁵⁸ A. C. A. Lee⁹³ G. R. Lee¹⁵ L. Lee⁵⁹
S. C. Lee¹⁴⁵ S. Lee⁷⁸ L. L. Leeuw^{31c} B. Lefebvre^{153a} H. P. Lefebvre⁹² M. Lefebvre¹⁶¹ C. Leggett^{16a}
K. Lehmann¹³⁹ N. Lehmann¹⁸ G. Lehmann Miotto³⁴ W. A. Leight⁴⁶ A. Leisos^{149,cc} M. A. L. Leite^{79d}
C. E. Leitgeb⁴⁶ R. Leitner¹³⁰ K. J. C. Leney⁴² T. Lenz²² S. Leone^{71a} C. Leonidopoulos⁵⁰ A. Leopold¹²⁴
C. Leroy¹⁰⁶ R. Les¹⁰⁵ C. G. Lester³⁰ M. Levchenko³⁵ J. Levêque⁴ D. Levin¹⁰⁴ L. J. Levinson¹⁶⁵
D. J. Lewis¹⁹ B. Li^{13b} B. Li^{60b} C. Li^{60a} C-Q. Li^{60c,60d} H. Li^{60a} H. Li^{60b} H. Li^{60b} J. Li^{60c} K. Li¹³⁵
L. Li^{60c} M. Li^{13a,13d} Q. Y. Li^{60a} S. Li^{60d,60c,dd} T. Li^{60b} X. Li⁴⁶ Y. Li⁴⁶ Z. Li^{60b} Z. Li¹²³ Z. Li¹⁰²
Z. Li⁸⁹ Z. Liang^{13a} M. Liberatore⁴⁶ B. Liberti^{73a} K. Lie^{62c} K. Lin¹⁰⁵ R. A. Linck⁶⁵ R. E. Lindley⁶
J. H. Lindon² A. Linss⁴⁶ E. Lipeles¹²⁵ A. Lipniacka¹⁵ T. M. Liss^{158,ee} A. Lister¹⁶⁰ J. D. Little⁷ B. Liu^{13a}
B. X. Liu¹³⁹ J. B. Liu^{60a} J. K. K. Liu³⁷ K. Liu^{60d,60c} M. Liu^{60a} M. Y. Liu^{60a} P. Liu^{13a} X. Liu^{60a} Y. Liu⁴⁶
Y. Liu^{13c,13d} Y. L. Liu¹⁰⁴ Y. W. Liu^{60a} M. Livan^{70a,70b} A. Lleres⁵⁸ J. Llorente Merino¹³⁹ S. L. Lloyd⁹¹
E. M. Lobodzinska⁴⁶ P. Loch⁶ S. Loffredo^{73a,73b} T. Lohse¹⁷ K. Lohwasser¹³⁶ M. Lokajicek^{128,a}
J. D. Long¹⁵⁸ I. Longarini^{72a,72b} L. Longo³⁴ R. Longo¹⁵⁸ I. Lopez Paz¹² A. Lopez Solis⁴⁶ J. Lorenz¹⁰⁷
N. Lorenzo Martinez⁴ A. M. Lory¹⁰⁷ A. Lösle⁵² X. Lou^{45a,45b} X. Lou^{13a,13d} A. Lounis⁶⁴ J. Love⁵
P. A. Love⁸⁸ J. J. Lozano Bahilo¹⁵⁹ G. Lu^{13a,13d} M. Lu^{60a} S. Lu¹²⁵ Y. J. Lu⁶³ H. J. Lubatti¹³⁵ C. Luci^{72a,72b}
F. L. Lucio Alves^{13c} A. Lucotte⁵⁸ F. Luehring⁶⁵ I. Luise¹⁴² L. Luminari^{72a} O. Lundberg¹⁴¹ B. Lund-Jensen¹⁴¹
N. A. Luongo¹²⁰ M. S. Lutz¹⁴⁸ D. Lynn²⁷ H. Lyons⁸⁹ R. Lysak¹²⁸ E. Lytken⁹⁵ F. Lyu^{13a} V. Lyubushkin³⁶
T. Lyubushkina³⁶ H. Ma²⁷ L. L. Ma^{60b} Y. Ma⁹³ D. M. Mac Donell¹⁶¹ G. Maccarrone⁵¹ C. M. Macdonald¹³⁶
J. C. MacDonald¹³⁶ R. Madar³⁸ W. F. Mader⁴⁸ M. Madugoda Ralalage Don¹¹⁸ N. Madysa⁴⁸ J. Maeda⁸¹
T. Maeno²⁷ M. Maerker⁴⁸ V. Magerl⁵² J. Magro^{66a,66c} D. J. Mahon³⁹ C. Maidantchik^{79b} A. Maio^{127a,127b,127d}
K. Maj^{82a} O. Majersky^{26a} S. Majewski¹²⁰ N. Makovec⁶⁴ B. Malaescu¹²⁴ Pa. Malecki⁸³ V. P. Maleev³⁵
F. Malek⁵⁸ D. Malito^{41b,41a} U. Mallik⁷⁷ C. Malone³⁰ S. Maltezos⁹ S. Malyukov³⁶ J. Mamuzic¹⁵⁹
G. Mancini⁵¹ J. P. Mandalia⁹¹ I. Mandić⁹⁰ L. Manhaes de Andrade Filho^{79a} I. M. Maniatis¹⁴⁹ M. Manisha¹³²
J. Manjarres Ramos⁴⁸ K. H. Mankinen⁹⁵ A. Mann¹⁰⁷ A. Manousos⁷⁶ B. Mansoulie¹³² I. Manthos¹⁴⁹
S. Manzoni¹¹² A. Marantis^{149,cc} G. Marchiori¹²⁴ M. Marcisovsky¹²⁸ L. Marcoccia^{73a,73b} C. Marcon⁹⁵
M. Marjanovic¹¹⁷ Z. Marshall^{16a} S. Marti-Garcia¹⁵⁹ T. A. Martin¹⁶³ V. J. Martin⁵⁰ B. Martin dit Latour¹⁵
L. Martinelli^{72a,72b} M. Martinez^{12,w} P. Martinez Agullo¹⁵⁹ V. I. Martinez Outschoorn¹⁰¹ S. Martin-Haugh¹³¹
V. S. Martoiu^{25b} A. C. Martyniuk⁹³ A. Marzin³⁴ S. R. Maschek¹⁰⁸ L. Masetti⁹⁸ T. Mashimo¹⁵⁰ J. Masik⁹⁹
A. L. Maslennikov³⁵ L. Massa^{21b} P. Massarotti^{69a,69b} P. Mastrandrea^{71a,71b} A. Mastroberardino^{41b,41a}
T. Masubuchi¹⁵⁰ D. Matakias²⁷ T. Mathisen¹⁵⁷ A. Matic¹⁰⁷ N. Matsuzawa¹⁵⁰ J. Maurer^{25b} B. Maček⁹⁰
D. A. Maximov³⁵ R. Mazini¹⁴⁵ I. Maznas¹⁴⁹ S. M. Mazza¹³³ C. Mc Ginn²⁷ J. P. Mc Gowan¹⁰²
S. P. Mc Kee¹⁰⁴ T. G. McCarthy¹⁰⁸ W. P. McCormack^{16a} E. F. McDonald¹⁰³ A. E. McDougall¹¹²
J. A. McFayden¹⁴³ G. Mchedlidze^{146b} M. A. McKay⁴² K. D. McLean¹⁶¹ S. J. McMahon¹³¹ P. C. McNamara¹⁰³
R. A. McPherson^{161,p} J. E. Mdhluli^{31f} Z. A. Meadows¹⁰¹ S. Meehan³⁴ T. Megy³⁸ S. Mehlhase¹⁰⁷
A. Mehta⁸⁹ B. Meirose⁴³ D. Melini¹⁴⁷ B. R. Mellado Garcia^{31f} A. H. Melo⁵³ F. Meloni⁴⁶ A. Melzer²²
E. D. Mendes Gouveia^{127a} A. M. Mendes Jacques Da Costa¹⁹ H. Y. Meng¹⁵² L. Meng³⁴ S. Menke¹⁰⁸

M. Mentink¹³⁴, E. Meoni^{41b,41a}, C. Merlassino¹²³, P. Mermod^{54,a}, L. Merola^{69a,69b}, C. Meroni^{68a,68b}, G. Merz,¹⁰⁴
 O. Meshkov³⁵, J. K. R. Meshreki¹³⁸, J. Metcalfe⁵, A. S. Mete⁵, C. Meyer⁶⁵, J-P. Meyer¹³², M. Michetti¹⁷,
 R. P. Middleton¹³¹, L. Mijović⁵⁰, G. Mikenberg¹⁶⁵, M. Mikesstikova¹²⁸, M. Mikuž⁹⁰, H. Mildner¹³⁶, A. Milic¹⁵²,
 C. D. Milke⁴², D. W. Miller³⁷, L. S. Miller³², A. Milov¹⁶⁵, D. A. Milstead^{45a,45b}, T. Min,^{13c} A. A. Minaenko³⁵,
 I. A. Minashvili^{146b}, L. Mince⁵⁷, A. I. Mincer¹¹⁴, B. Mindur^{82a}, M. Mineev³⁶, Y. Minegishi,¹⁵⁰ Y. Mino⁸⁴,
 L. M. Mir¹², M. Miralles Lopez¹⁵⁹, M. Mironova¹²³, T. Mitani¹⁶⁴, V. A. Mitsou¹⁵⁹, M. Mittal,^{60c} O. Miu¹⁵²,
 P. S. Miyagawa⁹¹, Y. Miyazaki,⁸⁶ A. Mizukami⁸⁰, J. U. Mjörnmark⁹⁵, T. Mkrtchyan^{61a}, M. Mlynarikova¹¹³,
 T. Moa^{45a,45b}, S. Mobius⁵³, K. Mochizuki¹⁰⁶, P. Moder⁴⁶, P. Mogg¹⁰⁷, A. F. Mohammed^{13a,13d}, S. Mohapatra³⁹,
 G. Mokgatitswane^{31f}, B. Mondal¹³⁸, S. Mondal¹²⁹, K. Mönig⁴⁶, E. Monnier¹⁰⁰, A. Montalbano¹³⁹,
 J. Montejo Berlingen³⁴, M. Montella¹¹⁶, F. Monticelli⁸⁷, N. Morange⁶⁴, A. L. Moreira De Carvalho^{127a},
 M. Moreno Llácer¹⁵⁹, C. Moreno Martinez¹², P. Morettini^{55b}, M. Morgenstern¹⁴⁷, S. Morgenstern¹⁶³, D. Mori¹³⁹,
 M. Morii⁵⁹, M. Morinaga¹⁵⁰, V. Morisbak¹²², A. K. Morley³⁴, A. P. Morris⁹³, L. Morvaj³⁴, P. Moschovakos³⁴,
 B. Moser¹¹², M. Mosidze^{146b}, T. Moskalets⁵², P. Moskvitina¹¹¹, J. Moss^{29,ff}, E. J. W. Moyses¹⁰¹, S. Muanza¹⁰⁰,
 J. Mueller¹²⁶, D. Muenstermann⁸⁸, R. Müller¹⁸, G. A. Mullier⁹⁵, J. J. Mullin,¹²⁵ D. P. Mungo^{68a,68b},
 J. L. Munoz Martinez¹², F. J. Munoz Sanchez⁹⁹, M. Murin⁹⁹, P. Murin^{26b}, W. J. Murray^{163,131}, A. Murrone^{68a,68b},
 J. M. Muse¹¹⁷, M. Muškinja^{16a}, C. Mwewa²⁷, A. G. Myagkov^{35,k}, A. J. Myers⁷, A. A. Myers,¹²⁶ G. Myers⁶⁵,
 M. Myska¹²⁹, B. P. Nachman^{16a}, O. Nackenhorst⁴⁷, A. Nag⁴⁸, K. Nagai¹²³, K. Nagano⁸⁰, J. L. Nagle²⁷,
 E. Nagy¹⁰⁰, A. M. Nairz³⁴, Y. Nakahama¹⁰⁹, K. Nakamura⁸⁰, H. Nanjo¹²¹, F. Napolitano^{61a}, R. Narayan⁴²,
 I. Naryshkin³⁵, M. Naseri³², C. Nass²², T. Naumann⁴⁶, G. Navarro^{20a}, J. Navarro-Gonzalez¹⁵⁹, R. Nayak¹⁴⁸,
 P. Y. Nechaeva³⁵, F. Nechansky⁴⁶, T. J. Neep¹⁹, A. Negri^{70a,70b}, M. Negrini^{21b}, C. Nellist¹¹¹, C. Nelson¹⁰²,
 K. Nelson¹⁰⁴, S. Nemecek¹²⁸, M. Nessi^{34,gg}, M. S. Neubauer¹⁵⁸, F. Neuhaus⁹⁸, J. Neundorff⁴⁶, R. Newhouse¹⁶⁰,
 P. R. Newman¹⁹, C. W. Ng¹²⁶, Y. S. Ng,¹⁷ Y. W. Y. Ng¹⁵⁶, B. Ngair^{33e}, H. D. N. Nguyen¹⁰⁰, R. B. Nickerson¹²³,
 R. Nicolaidou¹³², D. S. Nielsen⁴⁰, J. Nielsen¹³³, M. Niemeyer⁵³, N. Nikiforou¹⁰, V. Nikolaenko^{35,k},
 I. Nikolic-Audit¹²⁴, K. Nikolopoulos¹⁹, P. Nilsson²⁷, H. R. Nindhito⁵⁴, A. Nisati^{72a}, N. Nishu², R. Nisius¹⁰⁸,
 T. Nitta¹⁶⁴, T. Nobe¹⁵⁰, D. L. Noel³⁰, Y. Noguchi⁸⁴, I. Nomidis¹²⁴, M. A. Nomura,²⁷ M. B. Norfolk¹³⁶,
 R. R. B. Norisam⁹³, J. Novak⁹⁰, T. Novak⁴⁶, O. Novgorodova⁴⁸, L. Novotny¹²⁹, R. Novotny¹¹⁰, L. Nozka¹¹⁹,
 K. Ntekas¹⁵⁶, E. Nurse⁹³, F. G. Oakham^{32,f}, J. Ocariz¹²⁴, A. Ochi⁸¹, I. Ochoa^{127a}, J. P. Ochoa-Ricoux^{134a},
 S. Oda⁸⁶, S. Odaka⁸⁰, S. Oerdek¹⁵⁷, A. Ogrodnik^{82a}, A. Oh⁹⁹, C. C. Ohm¹⁴¹, H. Oide¹⁵¹, R. Oishi¹⁵⁰,
 M. L. Ojeda¹⁵², Y. Okazaki⁸⁴, M. W. O’Keefe,⁸⁹ Y. Okumura¹⁵⁰, A. Olariu,^{25b} L. F. Oleiro Seabra^{127a},
 S. A. Olivares Pino^{134d}, D. Oliveira Damazio²⁷, D. Oliveira Goncalves^{79a}, J. L. Oliver¹⁵⁶, M. J. R. Olsson¹⁵⁶,
 A. Olszewski⁸³, J. Olszowska^{83,a}, Ö. O. Öncel²², D. C. O’Neil¹³⁹, A. P. O’Neill¹²³, A. Onofre^{127a,127e},
 P. U. E. Onyisi¹⁰, R. G. Oreamuno Madriz,¹¹³ M. J. Oreglia³⁷, G. E. Orellana⁸⁷, D. Orestano^{74a,74b}, N. Orlando¹²,
 R. S. Orr¹⁵², V. O’Shea⁵⁷, R. Ospanov^{60a}, G. Otero y Garzon²⁸, H. Otono⁸⁶, P. S. Ott^{61a}, G. J. Ottino^{16a},
 M. Ouchrif^{33d}, J. Ouellette²⁷, F. Ould-Saada¹²², A. Ouraou^{132,a}, Q. Ouyang^{13a}, M. Owen⁵⁷, R. E. Owen¹³¹,
 K. Y. Oyulmaz^{11c}, V. E. Ozcan^{11c}, N. Ozturk⁷, S. Ozturk^{11c}, J. Pacalt¹¹⁹, H. A. Pacey³⁰, A. Pacheco Pages¹²,
 C. Padilla Aranda¹², S. Pagan Griso^{16a}, G. Palacino⁶⁵, S. Palazzo⁵⁰, S. Palestini³⁴, M. Palka^{82b}, P. Palmi^{82a},
 D. K. Panchal¹⁰, C. E. Pandini⁵⁴, J. G. Panduro Vazquez⁹², P. Pani⁴⁶, G. Panizzo^{66a,66c}, L. Paolozzi⁵⁴,
 C. Papadatos¹⁰⁶, S. Parajuli⁴², A. Paramonov⁵, C. Paraskevopoulos⁹, D. Paredes Hernandez^{62b}, B. Parida¹⁶⁵,
 T. H. Park¹⁵², A. J. Parker²⁹, M. A. Parker³⁰, F. Parodi^{55b,55a}, E. W. Parrish¹¹³, J. A. Parsons³⁹, U. Parzefall⁵²,
 L. Pascual Dominguez¹⁴⁸, V. R. Pascuzzi^{16a}, F. Pasquali¹¹², E. Pasqualucci^{72a}, S. Passaggio^{55b}, F. Pastore⁹²,
 P. Pasuwan^{45a,45b}, J. R. Pater⁹⁹, A. Pathak¹⁶⁶, J. Patton,⁸⁹ T. Pauly³⁴, J. Parkes¹⁴⁰, M. Pedersen¹²²,
 L. Pedraza Diaz¹¹¹, R. Pedro^{127a}, T. Peiffer⁵³, S. V. Peleganchuk³⁵, O. Penc¹²⁸, C. Peng^{62b}, H. Peng^{60a},
 M. Penzin³⁵, B. S. Peralva^{79a}, M. M. Perego⁶⁴, A. P. Pereira Peixoto^{127a}, L. Pereira Sanchez^{45a,45b},
 D. V. Perepelitsa²⁷, E. Perez Codina^{153a}, M. Perganti⁹, L. Perini^{68a,68b,a}, H. Pernegger³⁴, A. Perrevoort¹¹²,
 K. Peters⁴⁶, R. F. Y. Peters⁹⁹, B. A. Petersen³⁴, T. C. Petersen⁴⁰, E. Petit¹⁰⁰, V. Petousis¹²⁹, C. Petridou¹⁴⁹,
 P. Petroff⁶⁴, F. Petrucci^{74a,74b}, M. Pettee¹⁶⁸, N. E. Pettersson³⁴, K. Petukhova¹³⁰, A. Peyaud¹³², R. Pezoa^{134e},
 L. Pezzotti³⁴, G. Pezzullo¹⁶⁸, T. Pham¹⁰³, P. W. Phillips¹³¹, M. W. Phipps¹⁵⁸, G. Piacquadio¹⁴², E. Pianori^{16a},
 F. Piazza^{68a,68b}, A. Picazio¹⁰¹, R. Piegai²⁸, D. Pietreanu^{25b}, J. E. Pilcher³⁷, A. D. Pilkington⁹⁹,
 M. Pinamonti^{66a,66c}, J. L. Pinfold², C. Pitman Donaldson,⁹³ D. A. Pizzi³², L. Pizzimento^{73a,73b}, A. Pizzini¹¹²

- M.-A. Pleier²⁷ V. Plesanovs,⁵² V. Pleskot¹³⁰ E. Plotnikova,³⁶ P. Podberezko³⁵ R. Poettgen⁹⁵ R. Poggi⁵⁴
L. Poggioli¹²⁴ I. Pogrebnyak¹⁰⁵ D. Pohl²² I. Pokharel⁵³ G. Polesello^{70a} A. Poley^{139,153a} A. Policicchio^{72a,72b}
R. Polifka¹³⁰ A. Polini^{21b} C. S. Pollard¹²³ Z. B. Pollock¹¹⁶ V. Polychronakos²⁷ D. Ponomarenko³⁵
L. Pontecorvo³⁴ S. Popa^{25a} G. A. Popeneciu^{25d} L. Portales⁴ D. M. Portillo Quintero^{153a} S. Pospisil¹²⁹
P. Postolache^{25c} K. Potamianos¹²³ I. N. Potrap³⁶ C. J. Potter³⁰ H. Potti¹ T. Poulsen⁴⁶ J. Poveda¹⁵⁹
T. D. Powell¹³⁶ G. Pownall⁴⁶ M. E. Pozo Astigarraga³⁴ A. Prades Ibanez¹⁵⁹ P. Pralavorio¹⁰⁰ M. M. Prapa⁴⁴
S. Prell⁷⁸ D. Price⁹⁹ M. Primavera^{67a} M. A. Principe Martin⁹⁷ M. L. Proffitt¹³⁵ N. Proklova³⁵
K. Prokofiev^{62c} S. Protopopescu²⁷ J. Proudfoot⁵ M. Przybycien^{82a} D. Pudzha³⁵ P. Puzo,⁶⁴
D. Pyatiizbyantseva³⁵ J. Qian¹⁰⁴ Y. Qin⁹⁹ T. Qiu⁹¹ A. Quadt⁵³ M. Queitsch-Maitland³⁴
G. Rabanal Bolanos⁵⁹ F. Ragusa^{68a,68b} G. Rahal⁹⁶ J. A. Raine⁵⁴ S. Rajagopalan²⁷ K. Ran^{13a,13d}
D. F. Rassloff^{61a} D. M. Rauch⁴⁶ S. Rave⁹⁸ B. Ravina⁵⁷ I. Ravinovich¹⁶⁵ M. Raymond³⁴ A. L. Read¹²²
N. P. Readioff¹³⁶ D. M. Rebutzi^{70a,70b} G. Redlinger²⁷ K. Reeves⁴³ D. Reikher¹⁴⁸ A. Reiss⁹⁸ A. Rej¹³⁸
C. Rembser³⁴ A. Renardi⁴⁶ M. Renda^{25b} M. B. Rendel,¹⁰⁸ A. G. Rennie⁵⁷ S. Resconi^{68a} E. D. Resseguie^{16a}
S. Rettie⁹³ B. Reynolds,¹¹⁶ E. Reynolds¹⁹ M. Rezaei Estabragh¹⁶⁷ O. L. Rezanova³⁵ P. Reznicek¹³⁰
E. Ricci^{75a,75b} R. Richter¹⁰⁸ S. Richter⁴⁶ E. Richter-Was^{82b} M. Ridel¹²⁴ P. Rieck¹⁰⁸ P. Riedler³⁴ O. Rifki⁴⁶
M. Rijssenbeek¹⁴² A. Rimoldi^{70a,70b} M. Rimoldi⁴⁶ L. Rinaldi^{21b,21a} T. T. Rinn¹⁵⁸ M. P. Rinnagel¹⁰⁷
G. Ripellino¹⁴¹ I. Riu¹² P. Rivadeneira⁴⁶ J. C. Rivera Vergara¹⁶¹ F. Rizatdinova¹¹⁸ E. Rizvi⁹¹ C. Rizzi⁵⁴
B. A. Roberts¹⁶³ S. H. Robertson^{102,p} M. Robin⁴⁶ D. Robinson³⁰ C. M. Robles Gajardo,^{134e}
M. Robles Manzano⁹⁸ A. Robson⁵⁷ A. Rocchi^{73a,73b} C. Roda^{71a,71b} S. Rodriguez Bosca^{61a}
A. Rodriguez Rodriguez⁵² A. M. Rodríguez Vera^{153b} S. Roe,³⁴ A. R. Roepe-Gier¹¹⁷ J. Roggel¹⁶⁷ O. Røhne¹²²
R. A. Rojas^{134e} B. Roland⁵² C. P. A. Roland⁶⁵ J. Roloff²⁷ A. Romaniouk³⁵ M. Romano^{21b}
A. C. Romero Hernandez¹⁵⁸ N. Rompotis⁸⁹ M. Ronzani¹¹⁴ L. Roos¹²⁴ S. Rosati^{72a} B. J. Rosser¹²⁵
E. Rossi¹⁵² E. Rossi⁴ E. Rossi^{69a,69b} L. P. Rossi^{55b} L. Rossini⁴⁶ R. Rosten¹¹⁶ M. Rotaru^{25b} B. Rottler⁵²
D. Rousseau⁶⁴ D. Rousso³⁰ G. Rovelli^{70a,70b} A. Roy¹⁰ A. Rozanov¹⁰⁰ Y. Rozen¹⁴⁷ X. Ruan^{31f}
A. J. Ruby⁸⁹ T. A. Ruggeri,¹ F. Rühr⁵² A. Ruiz-Martinez¹⁵⁹ A. Rummler³⁴ Z. Rurikova⁵²
N. A. Rusakovich³⁶ H. L. Russell³⁴ L. Rustige³⁸ J. P. Rutherford⁶ E. M. Rüttinger¹³⁶ M. Rybar¹³⁰
E. B. Rye¹²² A. Ryzhov³⁵ J. A. Sabater Iglesias⁴⁶ P. Sabatini¹⁵⁹ L. Sabetta^{72a,72b} H. F.-W. Sadrozinski¹³³
F. Safai Tehrani^{72a} B. Safarzadeh Samani¹⁴³ M. Safdari¹⁴⁰ P. Saha¹¹³ S. Saha¹⁰² M. Sahinsoy¹⁰⁸ A. Sahu¹⁶⁷
M. Saimpert¹³² M. Saito¹⁵⁰ T. Saito¹⁵⁰ D. Salamani³⁴ G. Salamanna^{74a,74b} A. Salnikov¹⁴⁰ J. Salt¹⁵⁹
A. Salvador Salas¹² D. Salvatore^{41b,41a} F. Salvatore¹⁴³ A. Salzburger³⁴ D. Sammel⁵² D. Sampsonidis¹⁴⁹
D. Sampsonidou^{60d,60c} J. Sánchez¹⁵⁹ A. Sanchez Pineda⁴ V. Sanchez Sebastian¹⁵⁹ H. Sandaker¹²²
C. O. Sander⁴⁶ I. G. Sanderswood⁸⁸ J. A. Sandesara¹⁰¹ M. Sandhoff¹⁶⁷ C. Sandoval^{20b} D. P. C. Sankey¹³¹
M. Sannino^{55b,55a} Y. Sano¹⁰⁹ A. Sansoni⁵¹ C. Santoni³⁸ H. Santos^{127a,127b} S. N. Santpur^{16a} A. Santra¹⁶⁵
K. A. Saoucha¹³⁶ J. G. Saraiva^{127a,127d} J. Sardain¹⁰⁰ O. Sasaki⁸⁰ K. Sato¹⁵⁴ C. Sauer,^{61b} F. Sauerburger⁵²
E. Sauvan⁴ P. Savard^{152,f} R. Sawada¹⁵⁰ C. Sawyer¹³¹ L. Sawyer⁹⁴ I. Sayago Galvan,¹⁵⁹ C. Sbarra^{21b}
A. Sbrizzi^{66a,66c} T. Scanlon⁹³ J. Schaarschmidt¹³⁵ P. Schacht¹⁰⁸ D. Schaefer³⁷ U. Schäfer⁹⁸ A. C. Schaffer⁶⁴
D. Schaile¹⁰⁷ R. D. Schamberger¹⁴² E. Schanet¹⁰⁷ C. Scharf¹⁷ N. Scharmberg⁹⁹ V. A. Schegelsky³⁵
D. Scheirich¹³⁰ F. Schenck¹⁷ M. Schernau¹⁵⁶ C. Schiavi^{55b,55a} L. K. Schildgen²² Z. M. Schillaci²⁴
E. J. Schioppa^{67a,67b} M. Schioppa^{41b,41a} B. Schlag⁹⁸ K. E. Schleicher⁵² S. Schlenker³⁴ K. Schmieden⁹⁸
C. Schmitt⁹⁸ S. Schmitt⁴⁶ L. Schoeffel¹³² A. Schoening^{61b} P. G. Scholer⁵² E. Schopf¹²³ M. Schott⁹⁸
J. Schovancova³⁴ S. Schramm⁵⁴ F. Schroeder¹⁶⁷ H.-C. Schultz-Coulon^{61a} M. Schumacher⁵² B. A. Schumm¹³³
Ph. Schune¹³² A. Schwartzman¹⁴⁰ T. A. Schwarz¹⁰⁴ Ph. Schwemling¹³² R. Schwienhorst¹⁰⁵ A. Sciandra¹³³
G. Sciolla²⁴ F. Scuri^{71a} F. Scutti,¹⁰³ C. D. Sebastiani⁸⁹ K. Sedlaczek⁴⁷ P. Seema¹⁷ S. C. Seidel¹¹⁰
A. Seiden¹³³ B. D. Seidlitz²⁷ T. Seiss³⁷ C. Seitz⁴⁶ J. M. Seixas^{79b} G. Sekhniaidze^{69a} S. J. Sekula⁴²
L. Selem⁴ N. Semprini-Cesari^{21b,21a} S. Sen⁴⁹ C. Serfon²⁷ L. Serin⁶⁴ L. Serkin^{66a,66b} M. Sessa^{74a,74b}
H. Severini¹¹⁷ S. Sevova¹⁴⁰ F. Sforza^{55b,55a} A. Sfyrla⁵⁴ E. Shabalina⁵³ R. Shaheen¹⁴¹ J. D. Shahinian¹²⁵
N. W. Shaikh^{45a,45b} D. Shaked Renous¹⁶⁵ L. Y. Shan^{13a} M. Shapiro^{16a} A. Sharma³⁴ A. S. Sharma¹
S. Sharma⁴⁶ P. B. Shatalov³⁵ K. Shaw¹⁴³ S. M. Shaw⁹⁹ P. Sherwood⁹³ L. Shi⁹³ C. O. Shimmin¹⁶⁸
Y. Shimogama¹⁶⁴ J. D. Shinner⁹² I. P. J. Shipsey¹²³ S. Shirabe⁵⁴ M. Shiyakova^{36,hh} J. Shlomi¹⁶⁵

M. J. Shochet³⁷ J. Shojaii¹⁰³ D. R. Shope¹⁴¹ S. Shrestha¹¹⁶ E. M. Shrif^{31f} M. J. Shroff¹⁶¹ E. Shulga¹⁶⁵
 P. Sicho¹²⁸ A. M. Sickles¹⁵⁸ E. Sideras Haddad^{31f} O. Sidiropoulou³⁴ A. Sidoti^{21b} F. Siegert⁴⁸ Dj. Sijacki¹⁴
 J. M. Silva¹⁹ M. V. Silva Oliveira³⁴ S. B. Silverstein^{45a} S. Simion⁶⁴ R. Simoniello³⁴ S. Simsek^{11b}
 P. Sinervo¹⁵² V. Sinetckii³⁵ S. Singh¹³⁹ S. Singh¹⁵² S. Sinha⁴⁶ S. Sinha^{31f} M. Sioli^{21b,21a} I. Siral¹²⁰
 S. Yu. Sivoklokov^{35a} J. Sjölin^{45a,45b} A. Skaf⁵³ E. Skorda⁹⁵ P. Skubic¹¹⁷ M. Slawinska⁸³ K. Sliwa¹⁵⁵
 V. Smakhtin¹⁶⁵ B. H. Smart¹³¹ J. Smiesko¹³⁰ S. Yu. Smirnov³⁵ Y. Smirnov³⁵ L. N. Smirnova^{35,k}
 O. Smirnova⁹⁵ E. A. Smith³⁷ H. A. Smith¹²³ M. Smizanska⁸⁸ K. Smolek¹²⁹ A. Smykiewicz⁸³
 A. A. Snesev³⁵ H. L. Snoek¹¹² S. Snyder²⁷ R. Sobie^{161,p} A. Soffer¹⁴⁸ F. Sohns⁵³ C. A. Solans Sanchez³⁴
 E. Yu. Soldatov³⁵ U. Soldevila¹⁵⁹ A. A. Solodkov³⁵ S. Solomon⁵² A. Soloshenko³⁶ O. V. Solovyanov³⁵
 V. Solovyev³⁵ P. Sommer¹³⁶ H. Son¹⁵⁵ A. Sonay¹² W. Y. Song^{153b} A. Sopczak¹²⁹ A. L. Sopio⁹³
 F. Sopkova^{26b} S. Sottocornola^{70a,70b} R. Soualah^{66a,66c} Z. Soumami^{33e} D. South⁴⁶ S. Spagnolo^{67a,67b}
 M. Spalla¹⁰⁸ M. Spangenberg¹⁶³ F. Spanò⁹² D. Sperlich⁵² T. M. Spieker^{61a} G. Spigo³⁴ M. Spina¹⁴³
 D. P. Spiteri⁵⁷ M. Spousta¹³⁰ A. Stabile^{68a,68b} R. Stamen^{61a} M. Stamenkovic¹¹² A. Stampekis¹⁹
 M. Standke²² E. Stanecka⁸³ B. Stanislaus³⁴ M. M. Stanitzki⁴⁶ M. Stankaityte¹²³ B. Stapf⁴⁶
 E. A. Starchenko³⁵ G. H. Stark¹³³ J. Stark^{100,ii} D. M. Starko^{153b} P. Staroba¹²⁸ P. Starovoitov^{61a} S. Stärz¹⁰²
 R. Staszewski⁸³ G. Stavropoulos⁴⁴ P. Steinberg²⁷ A. L. Steinhebel¹²⁰ B. Stelzer^{139,153a} H. J. Stelzer¹²⁶
 O. Stelzer-Chilton^{153a} H. Stenzel⁵⁶ T. J. Stevenson¹⁴³ G. A. Stewart³⁴ M. C. Stockton³⁴ G. Stoicea^{25b}
 M. Stolarski^{127a} S. Stonjek¹⁰⁸ A. Straessner⁴⁸ J. Strandberg¹⁴¹ S. Strandberg^{45a,45b} M. Strauss¹¹⁷
 T. Streblner¹⁰⁰ P. Strizenec^{26b} R. Ströhmer¹⁶² D. M. Strom¹²⁰ L. R. Strom⁴⁶ R. Stroynowski⁴²
 A. Strubig^{45a,45b} S. A. Stucci²⁷ B. Stugu¹⁵ J. Stupak¹¹⁷ N. A. Styles⁴⁶ D. Su¹⁴⁰ S. Su^{60a} W. Su^{60d,135,60c}
 X. Su^{60a} N. B. Suarez¹²⁶ K. Sugizaki¹⁵⁰ V. V. Sulin³⁵ M. J. Sullivan⁸⁹ D. M. S. Sultan⁵⁴ S. Sultansoy^{3c}
 T. Sumida⁸⁴ S. Sun¹⁰⁴ S. Sun¹⁶⁶ X. Sun⁹⁹ O. Sunneborn Gudnadottir¹⁵⁷ C. J. E. Suster¹⁴⁴ M. R. Sutton¹⁴³
 M. Svatos¹²⁸ M. Swiatlowski^{153a} T. Swirski¹⁶² I. Sykora^{26a} M. Sykora¹³⁰ T. Sykora¹³⁰ D. Ta⁹⁸
 K. Tackmann^{46,ji} A. Taffard¹⁵⁶ R. Tafirout^{153a} E. Tagiev³⁵ R. H. M. Taibah¹²⁴ R. Takashima⁸⁵ K. Takeda⁸¹
 T. Takeshita¹³⁷ E. P. Takeva⁵⁰ Y. Takubo⁸⁰ M. Talby¹⁰⁰ A. A. Talyshev³⁵ K. C. Tam^{62b} N. M. Tamir¹⁴⁸
 A. Tanaka¹⁵⁰ J. Tanaka¹⁵⁰ R. Tanaka⁶⁴ Z. Tao¹⁶⁰ S. Tapia Araya⁷⁸ S. Tapprogge⁹⁸
 A. Tarek Abouelfadl Mohamed¹⁰⁵ S. Tarem¹⁴⁷ K. Tariq^{60b} G. Tarna^{25b,kk} G. F. Tartarelli^{68a} P. Tas¹³⁰
 M. Tasevsky¹²⁸ E. Tassi^{41b,41a} G. Tateno¹⁵⁰ Y. Tayalati^{33e} G. N. Taylor¹⁰³ W. Taylor^{153b} H. Teagle⁸⁹
 A. S. Tee¹⁶⁶ R. Teixeira De Lima¹⁴⁰ P. Teixeira-Dias⁹² H. Ten Kate³⁴ J. J. Teoh¹¹² K. Terashi¹⁵⁰ J. Terron⁹⁷
 S. Terzo¹² M. Testa⁵¹ R. J. Teuscher^{152,p} N. Themistokleous⁵⁰ T. Thevenaux-Pelzer¹⁷ O. Thielmann¹⁶⁷
 D. W. Thomas⁹² J. P. Thomas¹⁹ E. A. Thompson⁴⁶ P. D. Thompson¹⁹ E. Thomson¹²⁵ E. J. Thorpe⁹¹ Y. Tian⁵³
 V. Tikhomirov^{35,k} Yu. A. Tikhonov³⁵ S. Timoshenko³⁵ P. Tipton¹⁶⁸ S. Tisserant¹⁰⁰ S. H. Tlou^{31f} A. Tnourji³⁸
 K. Todome^{21b,21a} S. Todorova-Nova¹³⁰ S. Todt⁴⁸ M. Togawa⁸⁰ J. Tojo⁸⁶ S. Tokár^{26a} K. Tokushuku⁸⁰
 E. Tolley¹¹⁶ R. Tombs³⁰ M. Tomoto^{80,109} L. Tompkins^{140,ll} P. Tornambe¹⁰¹ E. Torrence¹²⁰ H. Torres⁴⁸
 E. Torró Pastor¹⁵⁹ M. Toscani²⁸ C. Toscirri³⁷ J. Toth^{100,mmm} D. R. Tovey¹³⁶ A. Traet¹⁵ C. J. Treado¹¹⁴
 T. Trefzger¹⁶² A. Tricoli²⁷ I. M. Trigger^{153a} S. Trincaz-Duvold¹²⁴ D. A. Trischuk¹⁶⁰ B. Trocmé⁵⁸
 A. Trofymov⁶⁴ C. Troncon^{68a} F. Trovato¹⁴³ L. Truong^{31c} M. Trzebinski⁸³ A. Trzupek⁸³ F. Tsai¹⁴²
 A. Tsiamis¹⁴⁹ P. V. Tsiareshka^{35,k} A. Tsirigotis^{149,cc} V. Tsiskaridze¹⁴² E. G. Tskhadadze^{146a} M. Tsopoulou¹⁴⁹
 I. I. Tsukerman³⁵ V. Tsulaia^{16a} S. Tsuno⁸⁰ O. Tsur¹⁴⁷ D. Tsybychev¹⁴² Y. Tu^{62b} A. Tudorache^{25b}
 V. Tudorache^{25b} A. N. Tuna³⁴ S. Turchikhin³⁶ I. Turk Cakir^{3b,nn} R. J. Turner¹⁹ R. Turra^{68a} P. M. Tuts³⁹
 S. Tzamarias¹⁴⁹ P. Tzani⁹ E. Tzovara⁹⁸ K. Uchida¹⁵⁰ F. Ukegawa¹⁵⁴ G. Unal³⁴ M. Unal¹⁰ A. Undrus²⁷
 G. Unel¹⁵⁶ F. C. Ungaro¹⁰³ K. Uno¹⁵⁰ J. Urban^{26b} P. Urquijo¹⁰³ G. Usai⁷ R. Ushioda¹⁵¹ M. Usman¹⁰⁶
 Z. Uysal^{11d} V. Vacek¹²⁹ B. Vachon¹⁰² K. O. H. Vadla¹²² T. Vafeiadis³⁴ C. Valderanis¹⁰⁷
 E. Valdes Santurio^{45a,45b} M. Valente^{153a} S. Valentinetti^{21b,21a} A. Valero¹⁵⁹ L. Valéry⁴⁶ R. A. Vallance¹⁹
 A. Vallier^{100,ii} J. A. Valls Ferrer¹⁵⁹ T. R. Van Daalen¹³⁵ P. Van Gemmeren⁵ S. Van Stroud⁹³ I. Van Vulpen¹¹²
 M. Vanadia^{73a,73b} W. Vandelli³⁴ M. Vandenbroucke¹³² E. R. Vandewall¹¹⁸ D. Vannicola¹⁴⁸ L. Vannoli^{55b,55a}
 R. Vari^{72a} E. W. Varnes⁶ C. Varni^{16a} T. Varol¹⁴⁵ D. Varouchas⁶⁴ K. E. Varvell¹⁴⁴ M. E. Vasile^{25b} L. Vaslin³⁸
 G. A. Vasquez¹⁶¹ F. Vazeille³⁸ D. Vazquez Furelos¹² T. Vazquez Schroeder³⁴ J. Veatch⁵³ V. Vecchio⁹⁹
 M. J. Veen¹¹² I. Veliscek¹²³ L. M. Veloce¹⁵² F. Veloso^{127a,127c} S. Veneziano^{72a} A. Ventura^{67a,67b}

A. Verbytskyi¹⁰⁸ M. Verducci^{71a,71b} C. Vergis²² M. Verissimo De Araujo^{79b} W. Verkerke¹¹²
A. T. Vermeulen¹¹² J. C. Vermeulen¹¹² C. Vernieri¹⁴⁰ P. J. Verschuuren⁹² M. L. Vesterbacka¹¹⁴
M. C. Vetterli^{139,f} A. Vgenopoulos¹⁴⁹ N. Viaux Maira^{134e} T. Vickey¹³⁶ O. E. Vickey Boeriu¹³⁶
G. H. A. Viehhauser¹²³ L. Vigani^{61b} M. Villa^{21b,21a} M. Villaplana Perez¹⁵⁹ E. M. Villhauer⁵⁰ E. Vilucchi⁵¹
M. G. Vinciter³² G. S. Virdee¹⁹ A. Vishwakarma⁵⁰ C. Vittori^{21b,21a} I. Vivarelli¹⁴³ V. Vladimirov¹⁶³
E. Voevodina¹⁰⁸ M. Vogel¹⁶⁷ P. Vokac¹²⁹ J. Von Ahnen⁴⁶ S. E. von Buddenbrock^{31f} E. Von Toerne²²
V. Vorobel¹³⁰ K. Vorobev³⁵ M. Vos¹⁵⁹ J. H. Vosseveld⁸⁹ M. Vozak⁹⁹ L. Vozdecky⁹¹ N. Vranjes¹⁴
M. Vranjes Milosavljevic¹⁴ V. Vrba^{129,a} M. Vreeswijk¹¹² R. Vuillermet³⁴ O. Vujanovic⁹⁸ I. Vukotic³⁷
S. Wada¹⁵⁴ C. Wagner¹⁰¹ W. Wagner¹⁶⁷ S. Wahdan¹⁶⁷ H. Wahlberg⁸⁷ R. Wakasa¹⁵⁴ M. Wakida¹⁰⁹
V. M. Walbrecht¹⁰⁸ J. Walder¹³¹ R. Walker¹⁰⁷ S. D. Walker⁹² W. Walkowiak¹³⁸ A. M. Wang⁵⁹ A. Z. Wang¹⁶⁶
C. Wang^{60a} C. Wang^{60c} H. Wang^{16a} J. Wang^{62a} P. Wang⁴² R.-J. Wang⁹⁸ R. Wang⁵⁹ R. Wang¹¹³
S. M. Wang¹⁴⁵ S. Wang^{60b} T. Wang^{60a} W. T. Wang^{60a} W. X. Wang^{60a} X. Wang^{13c} X. Wang¹⁵⁸ Y. Wang^{60a}
Z. Wang¹⁰⁴ A. Warburton¹⁰² C. P. Ward³⁰ R. J. Ward¹⁹ N. Warrack⁵⁷ A. T. Watson¹⁹ M. F. Watson¹⁹
G. Watts¹³⁵ B. M. Waugh⁹³ A. F. Webb¹⁰ C. Weber²⁷ M. S. Weber¹⁸ S. A. Weber³² S. M. Weber^{61a}
C. Wei^{60a} Y. Wei¹²³ A. R. Weidberg¹²³ J. Weingarten⁴⁷ M. Weirich⁹⁸ C. Weiser⁵² T. Wenaus²⁷
B. Wendland⁴⁷ T. Wengler³⁴ S. Wenig³⁴ N. Wermes²² M. Wessels^{61a} K. Whalen¹²⁰ A. M. Wharton⁸⁸
A. S. White⁵⁹ A. White⁷ M. J. White¹ D. Whiteson¹⁵⁶ L. Wickremasinghe¹²¹ W. Wiedenmann¹⁶⁶ C. Wiel⁴⁸
M. Wielers¹³¹ N. Wieseotte⁹⁸ C. Wiglesworth⁴⁰ L. A. M. Wiik-Fuchs⁵² D. J. Wilbern¹¹⁷ H. G. Wilkens³⁴
L. J. Wilkins⁹² D. M. Williams³⁹ H. H. Williams¹²⁵ S. Williams³⁰ S. Willocq¹⁰¹ P. J. Windischhofer¹²³
I. Wingerter-Seez⁴ F. Winklmeier¹²⁰ B. T. Winter⁵² M. Wittgen¹⁴⁰ M. Wobisch⁹⁴ A. Wolf⁹⁸ R. Wölker¹²³
J. Wollrath¹⁵⁶ M. W. Wolter⁸³ H. Wolters^{127a,127c} V. W. S. Wong¹⁶⁰ A. F. Wongel⁴⁶ S. D. Worm⁴⁶
B. K. Wosiek⁸³ K. W. Woźniak⁸³ K. Wraight⁵⁷ J. Wu^{13a,13d} S. L. Wu¹⁶⁶ X. Wu⁵⁴ Y. Wu^{60a} Z. Wu^{132,60a}
J. Wuerzinger¹²³ T. R. Wyatt⁹⁹ B. M. Wynne⁵⁰ S. Xella⁴⁰ M. Xia^{13b} J. Xiang^{62c} X. Xiao¹⁰⁴ M. Xie^{60a}
X. Xie^{60a} I. Xioidis¹⁴³ D. Xu^{13a} H. Xu^{60a} H. Xu^{60a} L. Xu^{60a} R. Xu¹²⁵ T. Xu^{60a} W. Xu¹⁰⁴ Y. Xu^{13b}
Z. Xu^{60b} Z. Xu¹⁴⁰ B. Yabsley¹⁴⁴ S. Yacoub^{31a} N. Yamaguchi⁸⁶ Y. Yamaguchi¹⁵¹ M. Yamatani¹⁵⁰
H. Yamauchi¹⁵⁴ T. Yamazaki^{16a} Y. Yamazaki⁸¹ J. Yan^{60c} S. Yan¹²³ Z. Yan²³ H. J. Yang^{60c,60d} H. T. Yang^{16a}
S. Yang^{60a} T. Yang^{62c} X. Yang^{60a} X. Yang^{13a} Y. Yang¹⁵⁰ Z. Yang^{60a,104} W-M. Yao^{16a} Y. C. Yap⁴⁶
H. Ye^{13c} J. Ye⁴² S. Ye²⁷ I. Yeletsikh³⁶ M. R. Yexley⁸⁸ P. Yin³⁹ K. Yorita¹⁶⁴ K. Yoshihara⁷⁸
C. J. S. Young⁵² C. Young¹⁴⁰ R. Yuan^{60b,oo} X. Yue^{61a} M. Zaazoua^{33e} B. Zabinski⁸³ G. Zacharis⁹ E. Zaid⁵⁰
T. Zakareishvili^{146b} N. Zakharchuk³² S. Zambito³⁴ D. Zanzi⁵² S. V. Zeiβner⁴⁷ C. Zeitnitz¹⁶⁷ J. C. Zeng¹⁵⁸
O. Zenin³⁵ T. Ženiš^{26a} S. Zenz⁹¹ S. Zerradi^{33a} D. Zerwas⁶⁴ M. Zgubič¹²³ B. Zhang^{13c} D. F. Zhang^{13b}
G. Zhang^{13b} J. Zhang⁵ K. Zhang^{13a,13d} L. Zhang^{13c} M. Zhang¹⁵⁸ R. Zhang¹⁶⁶ S. Zhang¹⁰⁴ X. Zhang^{60c}
X. Zhang^{60b} Z. Zhang⁶⁴ P. Zhao⁴⁹ Y. Zhao¹³³ Z. Zhao^{60a} A. Zhemchugov³⁶ Z. Zheng¹⁴⁰ D. Zhong¹⁵⁸
B. Zhou¹⁰⁴ C. Zhou¹⁶⁶ H. Zhou⁶ N. Zhou^{60c} Y. Zhou⁶ C. G. Zhu^{60b} C. Zhu^{13a,13d} H. L. Zhu^{60a} H. Zhu^{13a}
J. Zhu¹⁰⁴ Y. Zhu^{60a} X. Zhuang^{13a} K. Zhukov³⁵ V. Zhulanov³⁵ D. Zieminska⁶⁵ N. I. Zimine³⁶
S. Zimmermann^{52,a} J. Zinsser^{61b} M. Ziolkowski¹³⁸ L. Živković¹⁴ A. Zoccoli^{21b,21a} K. Zoch⁵⁴
T. G. Zorbas¹³⁶ O. Zormpa⁴⁴ W. Zou³⁹ and L. Zwalinski³⁴

(ATLAS Collaboration)

¹Department of Physics, University of Adelaide, Adelaide, Australia²Department of Physics, University of Alberta, Edmonton AB, Canada^{3a}Department of Physics, Ankara University, Ankara, Türkiye^{3b}Istanbul Aydin University, Application and Research Center for Advanced Studies, Istanbul, Türkiye^{3c}Division of Physics, TOBB University of Economics and Technology, Ankara, Türkiye⁴LAPP, Université Savoie Mont Blanc, CNRS/IN2P3, Annecy, France⁵High Energy Physics Division, Argonne National Laboratory, Argonne IL, United States of America⁶Department of Physics, University of Arizona, Tucson AZ, United States of America⁷Department of Physics, University of Texas at Arlington, Arlington TX, United States of America⁸Physics Department, National and Kapodistrian University of Athens, Athens, Greece⁹Physics Department, National Technical University of Athens, Zografou, Greece

- ¹⁰*Department of Physics, University of Texas at Austin, Austin TX, United States of America*
- ^{11a}*Bahcesehir University, Faculty of Engineering and Natural Sciences, Istanbul, Türkiye*
- ^{11b}*Istanbul Bilgi University, Faculty of Engineering and Natural Sciences, Istanbul, Türkiye*
- ^{11c}*Department of Physics, Bogazici University, Istanbul, Türkiye*
- ^{11d}*Department of Physics Engineering, Gaziantep University, Gaziantep, Türkiye*
- ¹²*Institut de Física d'Altes Energies (IFAE), Barcelona Institute of Science and Technology, Barcelona, Spain*
- ^{13a}*Institute of High Energy Physics, Chinese Academy of Sciences, Beijing, China*
- ^{13b}*Physics Department, Tsinghua University, Beijing, China*
- ^{13c}*Department of Physics, Nanjing University, Nanjing, China*
- ^{13d}*University of Chinese Academy of Science (UCAS), Beijing, China*
- ¹⁴*Institute of Physics, University of Belgrade, Belgrade, Serbia*
- ¹⁵*Department for Physics and Technology, University of Bergen, Bergen, Norway*
- ^{16a}*Physics Division, Lawrence Berkeley National Laboratory, Berkeley CA, United States of America*
- ^{16b}*University of California, Berkeley CA, United States of America*
- ¹⁷*Institut für Physik, Humboldt Universität zu Berlin, Berlin, Germany*
- ¹⁸*Albert Einstein Center for Fundamental Physics and Laboratory for High Energy Physics, University of Bern, Bern, Switzerland*
- ¹⁹*School of Physics and Astronomy, University of Birmingham, Birmingham, United Kingdom*
- ^{20a}*Facultad de Ciencias y Centro de Investigaciones, Universidad Antonio Nariño, Bogotá, Colombia*
- ^{20b}*Departamento de Física, Universidad Nacional de Colombia, Bogotá, Colombia*
- ^{21a}*Dipartimento di Fisica e Astronomia A. Righi, Università di Bologna, Bologna, Italy*
- ^{21b}*INFN Sezione di Bologna, Italy*
- ²²*Physikalisches Institut, Universität Bonn, Bonn, Germany*
- ²³*Department of Physics, Boston University, Boston MA, United States of America*
- ²⁴*Department of Physics, Brandeis University, Waltham MA, United States of America*
- ^{25a}*Transilvania University of Brasov, Brasov, Romania*
- ^{25b}*Horia Hulubei National Institute of Physics and Nuclear Engineering, Bucharest, Romania*
- ^{25c}*Department of Physics, Alexandru Ioan Cuza University of Iasi, Iasi, Romania*
- ^{25d}*National Institute for Research and Development of Isotopic and Molecular Technologies, Physics Department, Cluj-Napoca, Romania*
- ^{25e}*National University of Science and Technology Politehnica, Bucharest, Romania*
- ^{25f}*West University in Timisoara, Timisoara, Romania*
- ^{26a}*Faculty of Mathematics, Physics and Informatics, Comenius University, Bratislava, Slovak Republic*
- ^{26b}*Department of Subnuclear Physics, Institute of Experimental Physics of the Slovak Academy of Sciences, Kosice, Slovak Republic*
- ²⁷*Physics Department, Brookhaven National Laboratory, Upton NY, United States of America*
- ²⁸*Universidad de Buenos Aires, Facultad de Ciencias Exactas y Naturales, Departamento de Física, y CONICET, Instituto de Física de Buenos Aires (IFIBA), Buenos Aires, Argentina*
- ²⁹*California State University, CA, United States of America*
- ³⁰*Cavendish Laboratory, University of Cambridge, Cambridge, United Kingdom*
- ^{31a}*Department of Physics, University of Cape Town, Cape Town, South Africa*
- ^{31b}*Themba Labs, Western Cape, South Africa*
- ^{31c}*Department of Mechanical Engineering Science, University of Johannesburg, Johannesburg, South Africa*
- ^{31d}*National Institute of Physics, University of the Philippines Diliman (Philippines), Philippines*
- ^{31e}*University of South Africa, Department of Physics, Pretoria, South Africa*
- ^{31f}*School of Physics, University of the Witwatersrand, Johannesburg, South Africa*
- ³²*Department of Physics, Carleton University, Ottawa ON, Canada*
- ^{33a}*Faculté des Sciences Ain Chock, Réseau Universitaire de Physique des Hautes Energies—Université Hassan II, Casablanca, Morocco*
- ^{33b}*Faculté des Sciences, Université Ibn-Tofail, Kénitra, Morocco*
- ^{33c}*Faculté des Sciences Semlalia, Université Cadi Ayyad, LPHEA-Marrakech, Morocco*
- ^{33d}*LPMR, Faculté des Sciences, Université Mohamed Premier, Oujda, Morocco*
- ^{33e}*Faculté des sciences, Université Mohammed V, Rabat, Morocco*
- ³⁴*CERN, Geneva, Switzerland*
- ³⁵*Affiliated with an institute covered by a cooperation agreement with CERN*
- ³⁶*Affiliated with an international laboratory covered by a cooperation agreement with CERN*
- ³⁷*Enrico Fermi Institute, University of Chicago, Chicago IL, United States of America*
- ³⁸*LPC, Université Clermont Auvergne, CNRS/IN2P3, Clermont-Ferrand, France*

- ³⁹*Nevis Laboratory, Columbia University, Irvington NY, United States of America*
- ⁴⁰*Niels Bohr Institute, University of Copenhagen, Copenhagen, Denmark*
- ^{41a}*Dipartimento di Fisica, Università della Calabria, Rende, Italy*
- ^{41b}*INFN Gruppo Collegato di Cosenza, Laboratori Nazionali di Frascati, Italy*
- ⁴²*Physics Department, Southern Methodist University, Dallas TX, United States of America*
- ⁴³*Physics Department, University of Texas at Dallas, Richardson TX, United States of America*
- ⁴⁴*National Centre for Scientific Research “Demokritos”, Agia Paraskevi, Greece*
- ^{45a}*Department of Physics, Stockholm University, Sweden*
- ^{45b}*Oskar Klein Centre, Stockholm, Sweden*
- ⁴⁶*Deutsches Elektronen-Synchrotron DESY, Hamburg and Zeuthen, Germany*
- ⁴⁷*Fakultät Physik, Technische Universität Dortmund, Dortmund, Germany*
- ⁴⁸*Institut für Kern- und Teilchenphysik, Technische Universität Dresden, Dresden, Germany*
- ⁴⁹*Department of Physics, Duke University, Durham NC, United States of America*
- ⁵⁰*SUPA—School of Physics and Astronomy, University of Edinburgh, Edinburgh, United Kingdom*
- ⁵¹*INFN e Laboratori Nazionali di Frascati, Frascati, Italy*
- ⁵²*Physikalisches Institut, Albert-Ludwigs-Universität Freiburg, Freiburg, Germany*
- ⁵³*II. Physikalisches Institut, Georg-August-Universität Göttingen, Göttingen, Germany*
- ⁵⁴*Département de Physique Nucléaire et Corpusculaire, Université de Genève, Genève, Switzerland*
- ^{55a}*Dipartimento di Fisica, Università di Genova, Genova, Italy*
- ^{55b}*INFN Sezione di Genova, Italy*
- ⁵⁶*II. Physikalisches Institut, Justus-Liebig-Universität Giessen, Giessen, Germany*
- ⁵⁷*SUPA—School of Physics and Astronomy, University of Glasgow, Glasgow, United Kingdom*
- ⁵⁸*LPSC, Université Grenoble Alpes, CNRS/IN2P3, Grenoble INP, Grenoble, France*
- ⁵⁹*Laboratory for Particle Physics and Cosmology, Harvard University, Cambridge MA, United States of America*
- ^{60a}*Department of Modern Physics and State Key Laboratory of Particle Detection and Electronics, University of Science and Technology of China, Hefei, China*
- ^{60b}*Institute of Frontier and Interdisciplinary Science and Key Laboratory of Particle Physics and Particle Irradiation (MOE), Shandong University, Qingdao, China*
- ^{60c}*School of Physics and Astronomy, Shanghai Jiao Tong University, Key Laboratory for Particle Astrophysics and Cosmology (MOE), SKLPPC, Shanghai, China*
- ^{60d}*Tsung-Dao Lee Institute, Shanghai, China*
- ^{61a}*Kirchhoff-Institut für Physik, Ruprecht-Karls-Universität Heidelberg, Heidelberg, Germany*
- ^{61b}*Physikalisches Institut, Ruprecht-Karls-Universität Heidelberg, Heidelberg, Germany*
- ^{62a}*Department of Physics, Chinese University of Hong Kong, Shatin, N.T., Hong Kong, China*
- ^{62b}*Department of Physics, University of Hong Kong, Hong Kong, China*
- ^{62c}*Department of Physics and Institute for Advanced Study, Hong Kong University of Science and Technology, Clear Water Bay, Kowloon, Hong Kong, China*
- ⁶³*Department of Physics, National Tsing Hua University, Hsinchu, Taiwan*
- ⁶⁴*IJCLab, Université Paris-Saclay, CNRS/IN2P3, 91405, Orsay, France*
- ⁶⁵*Department of Physics, Indiana University, Bloomington IN, United States of America*
- ^{66a}*INFN Gruppo Collegato di Udine, Sezione di Trieste, Udine, Italy*
- ^{66b}*ICTP, Trieste, Italy*
- ^{66c}*Dipartimento Politecnico di Ingegneria e Architettura, Università di Udine, Udine, Italy*
- ^{67a}*INFN Sezione di Lecce, Italy*
- ^{67b}*Dipartimento di Matematica e Fisica, Università del Salento, Lecce, Italy*
- ^{68a}*INFN Sezione di Milano, Italy*
- ^{68b}*Dipartimento di Fisica, Università di Milano, Milano, Italy*
- ^{69a}*INFN Sezione di Napoli, Italy*
- ^{69b}*Dipartimento di Fisica, Università di Napoli, Napoli, Italy*
- ^{70a}*INFN Sezione di Pavia, Italy*
- ^{70b}*Dipartimento di Fisica, Università di Pavia, Pavia, Italy*
- ^{71a}*INFN Sezione di Pisa, Italy*
- ^{71b}*Dipartimento di Fisica E. Fermi, Università di Pisa, Pisa, Italy*
- ^{72a}*INFN Sezione di Roma, Italy*
- ^{72b}*Dipartimento di Fisica, Sapienza Università di Roma, Roma, Italy*
- ^{73a}*INFN Sezione di Roma Tor Vergata, Italy*
- ^{73b}*Dipartimento di Fisica, Università di Roma Tor Vergata, Roma, Italy*
- ^{74a}*INFN Sezione di Roma Tre, Italy*
- ^{74b}*Dipartimento di Matematica e Fisica, Università Roma Tre, Roma, Italy*

- ^{75a}INFN-TIFPA, Italy
- ^{75b}Università degli Studi di Trento, Trento, Italy
- ⁷⁶Universität Innsbruck, Department of Astro and Particle Physics, Innsbruck, Austria
- ⁷⁷University of Iowa, Iowa City IA, United States of America
- ⁷⁸Department of Physics and Astronomy, Iowa State University, Ames IA, United States of America
- ^{79a}Departamento de Engenharia Elétrica, Universidade Federal de Juiz de Fora (UFJF), Juiz de Fora, Brazil
- ^{79b}Universidade Federal do Rio De Janeiro COPPE/EE/IF, Rio de Janeiro, Brazil
- ^{79c}Universidade Federal de São João del Rei (UFSJ), São João del Rei, Brazil
- ^{79d}Instituto de Física, Universidade de São Paulo, São Paulo, Brazil
- ⁸⁰KEK, High Energy Accelerator Research Organization, Tsukuba, Japan
- ⁸¹Graduate School of Science, Kobe University, Kobe, Japan
- ^{82a}AGH University of Krakow, Faculty of Physics and Applied Computer Science, Krakow, Poland
- ^{82b}Marian Smoluchowski Institute of Physics, Jagiellonian University, Krakow, Poland
- ⁸³Institute of Nuclear Physics Polish Academy of Sciences, Krakow, Poland
- ⁸⁴Faculty of Science, Kyoto University, Kyoto, Japan
- ⁸⁵Kyoto University of Education, Kyoto, Japan
- ⁸⁶Research Center for Advanced Particle Physics and Department of Physics, Kyushu University, Fukuoka, Japan
- ⁸⁷Instituto de Física La Plata, Universidad Nacional de La Plata and CONICET, La Plata, Argentina
- ⁸⁸Physics Department, Lancaster University, Lancaster, United Kingdom
- ⁸⁹Oliver Lodge Laboratory, University of Liverpool, Liverpool, United Kingdom
- ⁹⁰Department of Experimental Particle Physics, Jožef Stefan Institute and Department of Physics, University of Ljubljana, Ljubljana, Slovenia
- ⁹¹School of Physics and Astronomy, Queen Mary University of London, London, United Kingdom
- ⁹²Department of Physics, Royal Holloway University of London, Egham, United Kingdom
- ⁹³Department of Physics and Astronomy, University College London, London, United Kingdom
- ⁹⁴Louisiana Tech University, Ruston LA, United States of America
- ⁹⁵Fysiska institutionen, Lunds universitet, Lund, Sweden
- ⁹⁶Centre de Calcul de l'Institut National de Physique Nucléaire et de Physique des Particules (IN2P3), Villeurbanne, France
- ⁹⁷Departamento de Física Teórica C-15 and CIAFF, Universidad Autónoma de Madrid, Madrid, Spain
- ⁹⁸Institut für Physik, Universität Mainz, Mainz, Germany
- ⁹⁹School of Physics and Astronomy, University of Manchester, Manchester, United Kingdom
- ¹⁰⁰CPPM, Aix-Marseille Université, CNRS/IN2P3, Marseille, France
- ¹⁰¹Department of Physics, University of Massachusetts, Amherst MA, United States of America
- ¹⁰²Department of Physics, McGill University, Montreal QC, Canada
- ¹⁰³School of Physics, University of Melbourne, Victoria, Australia
- ¹⁰⁴Department of Physics, University of Michigan, Ann Arbor MI, United States of America
- ¹⁰⁵Department of Physics and Astronomy, Michigan State University, East Lansing MI, United States of America
- ¹⁰⁶Group of Particle Physics, University of Montreal, Montreal QC, Canada
- ¹⁰⁷Fakultät für Physik, Ludwig-Maximilians-Universität München, München, Germany
- ¹⁰⁸Max-Planck-Institut für Physik (Werner-Heisenberg-Institut), München, Germany
- ¹⁰⁹Graduate School of Science and Kobayashi-Maskawa Institute, Nagoya University, Nagoya, Japan
- ¹¹⁰Department of Physics and Astronomy, University of New Mexico, Albuquerque NM, United States of America
- ¹¹¹Institute for Mathematics, Astrophysics and Particle Physics, Radboud University/Nikhef, Nijmegen, Netherlands
- ¹¹²Nikhef National Institute for Subatomic Physics and University of Amsterdam, Amsterdam, Netherlands
- ¹¹³Department of Physics, Northern Illinois University, DeKalb IL, United States of America
- ¹¹⁴Department of Physics, New York University, New York NY, United States of America
- ¹¹⁵Ochanomizu University, Otsuka, Bunkyo-ku, Tokyo, Japan
- ¹¹⁶Ohio State University, Columbus OH, United States of America
- ¹¹⁷Homer L. Dodge Department of Physics and Astronomy, University of Oklahoma, Norman OK, United States of America
- ¹¹⁸Department of Physics, Oklahoma State University, Stillwater OK, United States of America
- ¹¹⁹Palacký University, Joint Laboratory of Optics, Olomouc, Czech Republic
- ¹²⁰Institute for Fundamental Science, University of Oregon, Eugene, OR, United States of America
- ¹²¹Graduate School of Science, Osaka University, Osaka, Japan

- ¹²²*Department of Physics, University of Oslo, Oslo, Norway*
- ¹²³*Department of Physics, Oxford University, Oxford, United Kingdom*
- ¹²⁴*LPNHE, Sorbonne Université, Université Paris Cité, CNRS/IN2P3, Paris, France*
- ¹²⁵*Department of Physics, University of Pennsylvania, Philadelphia PA, United States of America*
- ¹²⁶*Department of Physics and Astronomy, University of Pittsburgh, Pittsburgh PA, United States of America*
- ^{127a}*Laboratório de Instrumentação e Física Experimental de Partículas—LIP, Lisboa, Portugal*
- ^{127b}*Departamento de Física, Faculdade de Ciências, Universidade de Lisboa, Lisboa, Portugal*
- ^{127c}*Departamento de Física, Universidade de Coimbra, Coimbra, Portugal*
- ^{127d}*Centro de Física Nuclear da Universidade de Lisboa, Lisboa, Portugal*
- ^{127e}*Departamento de Física, Universidade do Minho, Braga, Portugal*
- ^{127f}*Departamento de Física Teórica y del Cosmos, Universidad de Granada, Granada (Spain), Spain*
- ^{127g}*Dep Física and CEFITEC of Faculdade de Ciências e Tecnologia, Universidade Nova de Lisboa, Caparica, Portugal*
- ^{127h}*Departamento de Física, Instituto Superior Técnico, Universidade de Lisboa, Lisboa, Portugal*
- ¹²⁸*Institute of Physics of the Czech Academy of Sciences, Prague, Czech Republic*
- ¹²⁹*Czech Technical University in Prague, Prague, Czech Republic*
- ¹³⁰*Charles University, Faculty of Mathematics and Physics, Prague, Czech Republic*
- ¹³¹*Particle Physics Department, Rutherford Appleton Laboratory, Didcot, United Kingdom*
- ¹³²*IRFU, CEA, Université Paris-Saclay, Gif-sur-Yvette, France*
- ¹³³*Santa Cruz Institute for Particle Physics, University of California Santa Cruz, Santa Cruz CA, United States of America*
- ^{134a}*Departamento de Física, Pontificia Universidad Católica de Chile, Santiago, Chile*
- ^{134b}*Millennium Institute for Subatomic physics at high energy frontier (SAPHIR), Santiago, Chile*
- ^{134c}*Universidad Andres Bello, Department of Physics, Santiago, Chile*
- ^{134d}*Instituto de Alta Investigación, Universidad de Tarapacá, Arica, Chile*
- ^{134e}*Departamento de Física, Universidad Técnica Federico Santa María, Valparaíso, Chile*
- ¹³⁵*Department of Physics, University of Washington, Seattle WA, United States of America*
- ¹³⁶*Department of Physics and Astronomy, University of Sheffield, Sheffield, United Kingdom*
- ¹³⁷*Department of Physics, Shinshu University, Nagano, Japan*
- ¹³⁸*Department Physik, Universität Siegen, Siegen, Germany*
- ¹³⁹*Department of Physics, Simon Fraser University, Burnaby BC, Canada*
- ¹⁴⁰*SLAC National Accelerator Laboratory, Stanford CA, United States of America*
- ¹⁴¹*Department of Physics, Royal Institute of Technology, Stockholm, Sweden*
- ¹⁴²*Departments of Physics and Astronomy, Stony Brook University, Stony Brook NY, United States of America*
- ¹⁴³*Department of Physics and Astronomy, University of Sussex, Brighton, United Kingdom*
- ¹⁴⁴*School of Physics, University of Sydney, Sydney, Australia*
- ¹⁴⁵*Institute of Physics, Academia Sinica, Taipei, Taiwan*
- ^{146a}*E. Andronikashvili Institute of Physics, Iv. Javakhishvili Tbilisi State University, Tbilisi, Georgia*
- ^{146b}*High Energy Physics Institute, Tbilisi State University, Tbilisi, Georgia*
- ¹⁴⁷*Department of Physics, Technion, Israel Institute of Technology, Haifa, Israel*
- ¹⁴⁸*Raymond and Beverly Sackler School of Physics and Astronomy, Tel Aviv University, Tel Aviv, Israel*
- ¹⁴⁹*Department of Physics, Aristotle University of Thessaloniki, Thessaloniki, Greece*
- ¹⁵⁰*International Center for Elementary Particle Physics and Department of Physics, University of Tokyo, Tokyo, Japan*
- ¹⁵¹*Department of Physics, Tokyo Institute of Technology, Tokyo, Japan*
- ¹⁵²*Department of Physics, University of Toronto, Toronto ON, Canada*
- ^{153a}*TRIUMF, Vancouver BC, Canada*
- ^{153b}*Department of Physics and Astronomy, York University, Toronto ON, Canada*
- ¹⁵⁴*Division of Physics and Tomonaga Center for the History of the Universe, Faculty of Pure and Applied Sciences, University of Tsukuba, Tsukuba, Japan*
- ¹⁵⁵*Department of Physics and Astronomy, Tufts University, Medford MA, United States of America*
- ¹⁵⁶*Department of Physics and Astronomy, University of California Irvine, Irvine CA, United States of America*
- ¹⁵⁷*Department of Physics and Astronomy, University of Uppsala, Uppsala, Sweden*
- ¹⁵⁸*Department of Physics, University of Illinois, Urbana IL, United States of America*
- ¹⁵⁹*Instituto de Física Corpuscular (IFIC), Centro Mixto Universidad de Valencia—CSIC, Valencia, Spain*
- ¹⁶⁰*Department of Physics, University of British Columbia, Vancouver BC, Canada*
- ¹⁶¹*Department of Physics and Astronomy, University of Victoria, Victoria BC, Canada*

¹⁶²*Fakultät für Physik und Astronomie, Julius-Maximilians-Universität Würzburg, Würzburg, Germany*

¹⁶³*Department of Physics, University of Warwick, Coventry, United Kingdom*

¹⁶⁴*Waseda University, Tokyo, Japan*

¹⁶⁵*Department of Particle Physics and Astrophysics, Weizmann Institute of Science, Rehovot, Israel*

¹⁶⁶*Department of Physics, University of Wisconsin, Madison WI, United States of America*

¹⁶⁷*Fakultät für Mathematik und Naturwissenschaften, Fachgruppe Physik,*

Bergische Universität Wuppertal, Wuppertal, Germany

¹⁶⁸*Department of Physics, Yale University, New Haven CT, United States of America*

^aDeceased.

^bAlso at Department of Physics, King's College London, London, United Kingdom.

^cAlso at Istanbul University, Dept. of Physics, Istanbul, Türkiye.

^dAlso at Instituto de Fisica Teorica, IFT-UAM/CSIC, Madrid, Spain.

^eAlso at Institute of Physics, Azerbaijan Academy of Sciences, Baku, Azerbaijan.

^fAlso at TRIUMF, Vancouver BC, Canada.

^gAlso at Physics Department, An-Najah National University, Nablus, Palestine.

^hAlso at Department of Physics, University of Fribourg, Fribourg, Switzerland.

ⁱAlso at Department of Physics and Astronomy, University of Louisville, Louisville, KY, United States of America.

^jAlso at Departament de Fisica de la Universitat Autònoma de Barcelona, Barcelona, Spain.

^kAlso at Affiliated with an institute covered by a cooperation agreement with CERN.

^lAlso at The Collaborative Innovation Center of Quantum Matter (CICQM), Beijing, China.

^mAlso at Faculty of Physics, Sofia University, 'St. Kliment Ohridski', Sofia, Bulgaria.

ⁿAlso at Department of Physics, Ben Gurion University of the Negev, Beer Sheva, Israel.

^oAlso at Università di Napoli Parthenope, Napoli, Italy.

^pAlso at Institute of Particle Physics (IPP), Canada.

^qAlso at Bruno Kessler Foundation, Trento, Italy.

^rAlso at Borough of Manhattan Community College, City University of New York, New York NY, United States of America.

^sAlso at Department of Physics, California State University, Fresno, United States of America.

^tAlso at Department of Financial and Management Engineering, University of the Aegean, Chios, Greece.

^uAlso at Centro Studi e Ricerche Enrico Fermi, Italy.

^vAlso at Department of Physics, California State University, East Bay, United States of America.

^wAlso at Institutio Catalana de Recerca i Estudis Avancats, ICREA, Barcelona, Spain.

^xAlso at Physikalisches Institut, Albert-Ludwigs-Universität Freiburg, Freiburg, Germany.

^yAlso at University of Chinese Academy of Sciences (UCAS), Beijing, China.

^zAlso at Yeditepe University, Physics Department, Istanbul, Türkiye.

^{aa}Also at Institute of Theoretical Physics, Iliia State University, Tbilisi, Georgia.

^{bb}Also at CERN, Geneva, Switzerland.

^{cc}Also at Hellenic Open University, Patras, Greece.

^{dd}Also at Center for High Energy Physics, Peking University, China.

^{ee}Also at The City College of New York, New York NY, United States of America.

^{ff}Also at Department of Physics, California State University, Sacramento, United States of America.

^{gg}Also at Département de Physique Nucléaire et Corpusculaire, Université de Genève, Genève, Switzerland.

^{hh}Also at Institute for Nuclear Research and Nuclear Energy (INRNE) of the Bulgarian Academy of Sciences, Sofia, Bulgaria.

ⁱⁱAlso at L2IT, Université de Toulouse, CNRS/IN2P3, UPS, Toulouse, France.

^{jj}Also at Institut für Experimentalphysik, Universität Hamburg, Hamburg, Germany.

^{kk}Also at CPPM, Aix-Marseille Université, CNRS/IN2P3, Marseille, France.

^{ll}Also at Department of Physics, Stanford University, Stanford CA, United States of America.

^{mmm}Also at Institute for Particle and Nuclear Physics, Wigner Research Centre for Physics, Budapest, Hungary.

ⁿⁿAlso at Giresun University, Faculty of Engineering, Giresun, Türkiye.

^{oo}Also at Department of Physics and Astronomy, Michigan State University, East Lansing MI, United States of America.